Regulation of Transporters by Perfluorinated Carboxylic Acids in HepaRG Cells

Youjun Park Suh

A thesis

submitted in partial fulfillment of the

requirements for the degree of

Master of Science

University of Washington

2022

Reading Committee:

Julia Yue Cui

Elaine Faustman

Program Authorized to Offer Degree:

Environmental & Occupational Health Sciences

University of Washington

Abstract

Regulation of Transporters by Perfluorinated Carboxylic Acids in HepaRG cells

Youjun Park Suh

Chair of the Supervisory Committee:

Julia Yue Cui

Elaine Faustman

Department of Environmental & Occupational Health Sciences

Perfluorinated carboxylic acids (PFCAs) are widespread environmental pollutants for which human exposure has been documented. PFCAs at high doses were known to regulate xenobiotic transporters partly through PPARα and CAR in rodent models. Less is known regarding how various PFCAs at a lower concentration modulate transporters for endogenous substrates such as amino acids in human hepatocytes. Such studies are of particular importance because amino acids are involved in chemical detoxification and their transport system may serve as promising therapeutic targets for structurally similar xenobiotics. The focus of this study was to further elucidate how PFCAs modulate transporters involved in intermediary metabolism and xenobiotic biotransformation. We tested the hepatic transcriptomic response of HepaRG cells exposed to 45 μM of PFOA, PFNA, or PFDA in triplicates for 24 hours (vehicle: 0.1% DMSO), as well as the

prototypical ligands for PPARα (WY-14643, 45 μM) and CAR (CITCO, 2 μM). PFCAs with increasing carbon chain lengths (C8-C10) regulated more liver genes, with amino acid metabolism and transport ranked among the top enriched pathways and PFDA ranked as the most potent PFCA tested. Genes encoding amino acid transporters, which are essential for protein synthesis, were novel inducible targets by all 3 PFCAs, suggesting a potentially protective mechanism to reduce further toxic insults. None of the transporter regulations appeared to be through PPARα or CAR but potential involvement of Nrf2 is noted for all 3 PFCAs. In conclusion, PFCAs with increasing carbon chain lengths up-regulate amino acid transporters and modulate xenobiotic transporters to limit further toxic exposures in HepaRG cells.

TABLE OF CONTENTS

INTRODUCTION

Perfluorinated carboxylic acids (PFCAs) have been extensively used in many consumer products such as Scotchgard and the Teflon brand products due to their chemical and thermal stability. PFCAs such as perfluorooctanoic acid (PFOA, C8), PFNA (perfluorononanoic acid, C9), and perfluorodecanoic acid (PFDA, C10) have raised increasing public health concerns due to their highly persistent and bio-accumulative nature, and have been detected in ecosystems (Falandysz et al., 2006; Sinclair et al., 2006)(Smithwick et al., 2005; Calafat et al., 2006; De Silva and Mabury, 2006; Eggers Pedersen et al., 2015; Pasanisi et al., 2016; Boisvert et al., 2019; Jarvis et al., 2021).

Due to both tissue binding and uptake (Fujii et al., 2015; Van Rafelghem et al.,1987; Vanden Heuvel et al.,1991a; Vanden Heuvel et al., 1991b), the liver is one of the primary target organs of the toxic effects of PFCAs including oxidative stress, hepatomegaly, and hepatic dyslipidemia as described in detail below (Fujii et al., 2015). The solute carrier organic anion (SLCO) transporters, also known as the organic anion transporting polypeptides (OATP), are involved in the cellular uptake of many drugs and other chemicals (Hagenbuch and Meier, 2004). Using transfected Chinese hamster ovary and human embryonic kidney 293 cells, it was shown that the human OATP1B1, 1B3, and 2B1 can transport PFOA and PFNA (Zhao et al., 2017). An active uptake mechanism for the anion of PFOA (PFO) was also identified in rat hepatocytes (Han et al., 2008), although the exact transporters involved need to be further investigated.

The nuclear receptors pregnane X receptor (PXR/NR1I2), constitutive androstane receptor (CAR/NRI13), peroxisome proliferator-activated receptor α (PPARα), as well as the

transcription factors aryl hydrocarbon receptor (AhR) and nuclear factor erythroid 2-related factor 2 (NRF2) are widely recognized xenobiotic-sensing receptors that transcriptionally modulate various drug-processing genes (Aleksunes and Klaassen, 2012; Cui and Klaassen, 2016; Li et al., 2016). Previous studies on PFCAs have shown that they can activate distinct xenobiotic-sensing receptors such as CAR and PPARα in a dose- and congener-dependent manner; while most of these observations were from laboratory rodent models (Kudo and Kawashima, 2003; Maher et al., 2005; Cheng and Klaassen, 2008a; Cheng and Klaassen, 2008b; Oshida et al., 2015; Wen et al., 2019), a few studies have also tested the effect of PFCAs on human liver cancer-derived HepaRG cells (Buhrke et al., 2013; Abe et al., 2017; Behr et al., 2020; Louisse et al., 2020). Specifically, PFOA, PFNA, and PFDA have been shown to activate PPARα, with PFOA having the highest potential of PPARα activation, whereas these PFCA compounds also activate PPARγ and PPARδ with a much weaker potential (Buhrke et al., 2013; Li et al., 2020). PFOA also activates CAR in both mouse liver and HepaRG cells (Abe et al., 2017).

While most studies on PFCAs have focused on drug metabolizing enzymes and the pathological outcomes in human hepatocyte and rodent models, a systematic characterization of all transporters by PFCAs in human hepatocytes is lacking, especially the transporters for endogenous metabolites. In addition, only two studies have investigated PFCAs (PFOA and PFNA) and HepaRG cells, both of which used higher concentrations (Behr et al., 2020; Louisse et al., 2020), and there is no information regarding how PFDA modulates transporters in HepaRG cells. Therefore, the goal of this study was to fill these critical knowledge gaps. To note, it is important to investigate the effect of PFCAs on not only the drug transporters but also

the transporters involved in physiological functions such as nutrition, because it is increasingly recognized that environmental toxicant exposure may impact intermediary metabolism and lead to complex metabolic diseases (Lubrano et al., 2013; Heindel et al., 2017; Le Magueresse-Battistoni et al., 2018; Pannala et al., 2020). We also aimed to determine the effect of various equimolar PFCA congeners at non-toxic concentrations on the global transcriptomic response in human hepatocytes to unveil upstream regulators of transporters as well as early toxicological biomarkers in an unbiased manner. We also conducted a systematic comparison between our findings on PFCA-mediated transporter regulation in HepaRG cells and the literature in a dose- and congener-specific manner. The transporter genes included within the scope of the present study are shown in Supplemental Table 1.

MATERIALS AND METHODS (the overall study design is shown in Fig. 1A)

HepaRG cell culture and chemical exposure

We obtained the HepaRG cells from Biopedric with permission under the material and transfer agreement (MTA). The HepaRG cells were seeded at a density of $2.6 \times 10^4/cm^2$ in six-well plates (Tissue Culture Treated, Corning 3516) in William's medium E supplemented with a growth medium supplement (Catalog #ADD711, Triangle Research Labs, NC), GlutaMAX-I (1X), as well as penicillin (100 IU/ml) and streptomycin (100 μg/ml). To differentiate the HepaRG cells into a hepatocyte-like morphology, two weeks post-seeding, cells were transferred to new plates containing the same medium with a differentiation medium supplement (Catalog #

ADD721, Triangle Research Labs, NC), as well as penicillin (100 IU/ml) and streptomycin (100 μg/ml). The cells were cultured under this differentiation condition for another two weeks, and the medium was renewed every 2 or 3 days. Prior to the exposure to chemicals, the cell culture medium was switched to the Williams' medium E with induction supplement (HPRG740, Life Technologies, Carlsbad, CA) for 24 hours. The fully differentiated HepaRG cells were then exposed for 24 hours in triplicates to vehicle (0.1% DMSO), the selective CAR agonist CITCO (6-(4-Chlorophenyl)imidazo[2,1-b][1,3]thiazole-5-carbaldehyde O-(3,4-dichlorobenzyl)oxime, $C_{19}H_{12}N_3OCl_3S$, CAS Number 338404-52-7, Sigma-Aldrich, Catalog No. C6240, 2 μM), the selective PPARα agonist WY-14643 (4-Chloro-6-(2,3-xylidino)-2-pyrimidinylthioacetic acid, $C_{14}H_{14}ClN_3O_2S$, CAS Number: 50892-23-4, Sigma-Aldrich, Catalog No. C7081, 45 μM), PFOA (perfluorooctanoic acid; CAS Number: 335-67-1; $CF_3(CF_2)_6COOH$; Sigma-Aldrich, Catalog No. 171468; 45 μM), PFDA (perfluorodecanoic acid; CAS Number: 335-76-2; $CF_3(CF_2)_8CO_2H$; Sigma-Aldrich, Catalog No. 17741; 45 μM), or PFNA (perfluorononanoic acid; CAS Number: 375-95-1; $CF_3(CF_2)_7COOH$, Sigma-Aldrich, Catalog No. 394459; 45 μM). The concentration of PFCAs (45 μM) was selected based on literature evidence of no or minimal cellular toxicity, and up-regulation of CAR- and PPARα-targeted P450s (Buhrke et al., 2013; Abe et al., 2017; Behr et al., 2020; Louisse et al., 2020). Specifically, regarding HepaRG cell viability, PFOA exposure for 24 hours remained non-toxic even at a concentraion as high as 750 μM, which is the highest concentration tested (Behr et al., 2020); PFNA exposure for 24 hours remained non-toxic at 100 μM, whereas a decrease in cell viability was observed at 200 μM and above (Louisse et al., 2020). The HepaRG cell viability at 24 hours PFDA exposure was not known, however, it has been demonstrated that in HepaRG cells, which is another liver cancer-derived cell line, the IC50

at 72 hours post PFDA exposure was 15 μM (Buhrke et al., 2013). However, it is known that prolonged incubation of HepaRG cells with PFCAs results in greater reduction of cell viability (Louisse et al., 2020), and HepG2 cells are more sensitive than HepaRG cells to PFCA-induced toxicity at the same concentration and exposure time (Buhrke et al., 2013; Louisse et al., 2020). While it has been reported that there is a correlation between the cytotoxicity potential of a PFCA compound and its carbon chain length at high concentrations and prolonged incubation time points (Buhrke et al., 2013), we did not expect cellular toxicity at the low concentration of 45 μM PFDA at 24 hours. Regarding CAR- and PPARα -signaling, it has been shown that 48 hours incubation of PFOA up-regulated cytochrome P450 family 2 subfamily B member 6 (CYP2B6, CAR-target gene) and cytochrome P450 family 4 subfamily A member 11 (CYP4A11, PPARα -target gene), whereas the up-regulation was lost at 100 μM (Abe et al., 2017); thus, at 24 hours, we expect that a slightly higher concentration is required but it needs to be below 100 μM. Therefore, given the literature evidence of the effect of PFCA concentrations and incubation time on cellular toxicity and nuclear receptor activation, we selected 45 μM for all 3 PFCAs. All 3 PFCA congeners were set at equal molar concentrations to compare the potency in modulating the transporter gene expression and the general impact on the hepatic transcriptomic response. The selection of the CITCO and WY-14643 concentrations was based on the observations of the mRNA up-regulation of the prototypical CAR- and PPARα target genes (Fig. S1).

RNA isolation

Cells were washed with PBS and re-suspended in RNA-Bee reagent (Tel-Test Inc., Friendswood, Texas). RNA was isolated using RNA-Bee reagent (Tel-Test Inc., Friendswood, Texas, Catalog No. CS-501B, 1 ml/well), according to the manufacturers' instructions. RNA concentrations were quantified using a NanoDrop 1000 Spectrophotometer (Thermo Scientific, Waltham, MA) at 260 nm. The RNA integrity was assessed by visualizing the 18S and 28S rRNA bands under UV light using formaldehyde-agarose gel electrophoresis. In addition, an Agilent 2100 Bioanalyzer (Agilent Technologies Inc., Santa Clara, CA) was used to quantify the concentration of the RNA samples and confirm the RNA integrity. Samples with RNA integrity numbers (RIN) above 8.0 were used for RNA-Seq.

Reverse transcription and quantitative polymerase chain reaction (RT-qPCR)

Total RNA was reversely transcribed into cDNA using the High-Capacity cDNA Reverse Transcription Kit (Life Technologies, Carlsbad, CA). The resulting cDNA products were amplified by qPCR using the SsoAdvanced^{TM} Universal SYBR Green Supermix in a Bio-Rad CFX384 Real-Time PCR Detection System (Bio-Rad, Hercules, CA). The primers for all qPCR reactions were synthesized by Integrated DNA Technologies (Coralville, IA), and primer sequences are shown in Supplemental Table 2. Data are expressed as % of the expression of the housekeeping gene GAPDH. Differential expression was determined by one-way analysis of variance (ANOVA) followed by Duncan's post hoc test ($p < 0.05$).

RNA sequencing

In triplicates, the cDNA library was constructed using an Illumina TruSeq Stranded mRNA kit (Illumina, San Diego, CA) using the poly-A tail selection strategy. The RNA fragmentation, first and second strand cDNA syntheses, end repair, adaptor ligation, and PCR amplification were performed according to the manufacturer's protocol. The cDNA libraries were then validated for quantity and integrity using an Agilent 2100 Bioanalyzer (Agilent Technologies Inc., Santa Clara, CA) before sequencing. Reads were sequenced using a 50 bp paired-end sequencing per the Illumina manufacturer's protocol. The FASTQ files were de-multiplexed and concatenated for each sample. Quality control of the FASTQ files was performed using FastQC (http://www.bioinformatics.babraham.ac.uk/projects/fastqc/). Sequenced reads from the FASTQ files were then mapped to the human reference genome (National Center for Biotechnology Information [NCBI GRCh38 Ensembl 103]) using HISAT2 version 2.1 (Kim et al., 2019). The sequencing alignment/map (SAM) files were converted and sorted to binary alignment/map (BAM) format using SAMtools version 1.8 (Li et al., 2009). BAM files were converted to count files by featureCounts using the GRCh38.103.gtf. The raw and analyzed RNA-Seq data are deposited to the NCBI GEO database.

Data analysis

Differential expression analysis was performed using DESeq2 (Love et al., 2014). The differentially expressed genes were defined as having a false discovery rate - Benjamini-

Hochberg adjusted *p*-value (FDR-BH) < 0.05 in the chemical-exposed groups as compared to the vehicle-exposed control group. Up- or down-regulated genes were defined as having an absolute fold change (chemical exposed group over vehicle-exposed group) greater than 1.5. Differentially regulated genes were overlapped with a reference KEGG database containing genes of specific categories of functions, namely xenobiotic biotransformation, transcription factors, oxidative stress, and inflammation. Venn diagrams were plotted for differentially regulated genes comparing different exposure groups using the R package VennDiagram (Chen and Boutros, 2011). Hierarchical clustering was performed on all differentially expressed genes using the R package ComplexHeatmap (Gu et al., 2016). Lists of up- and down-regulated genes were used as input for gene ontology enrichment using the R package topGO (Alexa and Rahnenfuhrer, 2021), and the list of genes in the unfiltered expression table was used as the background. RNA-seq count matrix was normalized to transcripts per million (TPM). Genes were considered expressed if the transcripts per million (TPM) of each gene were greater than the total sample number and if the variance was greater than 1. Up- and down-regulated genes, as well as transporters were subject to upstream regulator prediction with adjusted p-value less than 0.1 using the enrichR function on the TRRUST Transcription factor database (Chen et al., 2013; Han et al., 2018). Bar plots and box and whiskers plots were created using ggplot2 (Wickham, 2016).

Transporter gene selection and visualization

Within the transporter superfamily, there are two major clusters of transporter genes in humans and rodents, namely the transport ATPases (including P, V, F, and ABC families) and the solute carrier (SLC) families (Pedersen, 2005; Doring and Petzinger, 2014). Based on the literature, the transporters investigated in this study are summarized in Supplemental Table 1. Individual differentially regulated transporter genes were plotted using Sigma Plot (SPSS Inc., Chicago, IL).

RESULTS

Effect of PFCA exposure on the hepatic transcriptomic changes in HepaRG cells

To assess how exposure to various PFCAs modulate the hepatic transcriptome in HepaRG cells, RNA-Seq was performed in DMSO-, PFOA-, PFNA-, and PFDA-exposed HepaRG cells (n=3 per group) as described in MATERIALS AND METHODS. Because it is known that PFCAs activate the nuclear receptors PPARα and CAR, as a positive control, HepaRG cells exposed to the prototypical PPARα ligand (WY-14643, abbreviated as "WY") and the prototypical CAR ligand (CITCO) were also included (n=2 per group). As shown in Supplemental Fig. 1, selected members of the first 4 CYP families were tested as positive controls for the effects of the prototypical PPARα and CAR ligands as well as PFCAs by RT-qPCR. At the selected concentrations, CITCO was the only chemical that up-regulated the

mRNA of CYP1A2, which is a prototypical AhR-target gene but can also be up-regulated by CAR activation. The prototypical CAR-target gene CYP2B6 mRNA was up-regulated by CITCO and all 3 PFCAs but not altered by WY. The mRNA of CYP3A4 was up-regulated by CITCO and tended to be up-regulated by the other chemicals but was not statistically significant. To note, CYP3A4 is a prototypical PXR-target gene but can also be up-regulated by CAR activation. The mRNA of the prototypical PPARα-target gene CYP4A11 was up-regulated by WY and all 3 PFCAs but not by CITCO (Supplemental Fig. S1). In summary, as expected, the prototypical ligands activated the corresponding nuclear receptors, whereas all PFCAs appeared to activate CAR and PPARα but not AhR, whereas a moderate trend of PXR-activation was noted but was not statistically significant.

As shown in Fig. 1B-1F, principal component analysis (PCA) was performed on the normalized, filtered, and Z-transformed gene expression matrix. For all exposures, the first two principal components (PCs) explained at least 85% of the total variation in the filtered gene expression matrix. All PC1 and PC2 explained 78% of the total variation in the combined exposure groups of liver cells (Supplemental Fig. 2A). PFCAs tended to be clustered together, apart from DMSO (Fig. S2A). The coordinates of the WY- and CITCO-exposed groups tended to be clustered together, although no clear groups were observed (Fig. 1B and 1C). On the contrary, HepaRG cells exposed to PFOA, PFNA, or PFDA clustered distinctly from the DMSO-exposed control group (Fig. 1D-1F), suggesting that the PFCA exposure resulted in greater transcriptomic differences than the exposure to prototypical nuclear receptor ligands, likely through PARα/CAR-independent mechanisms.

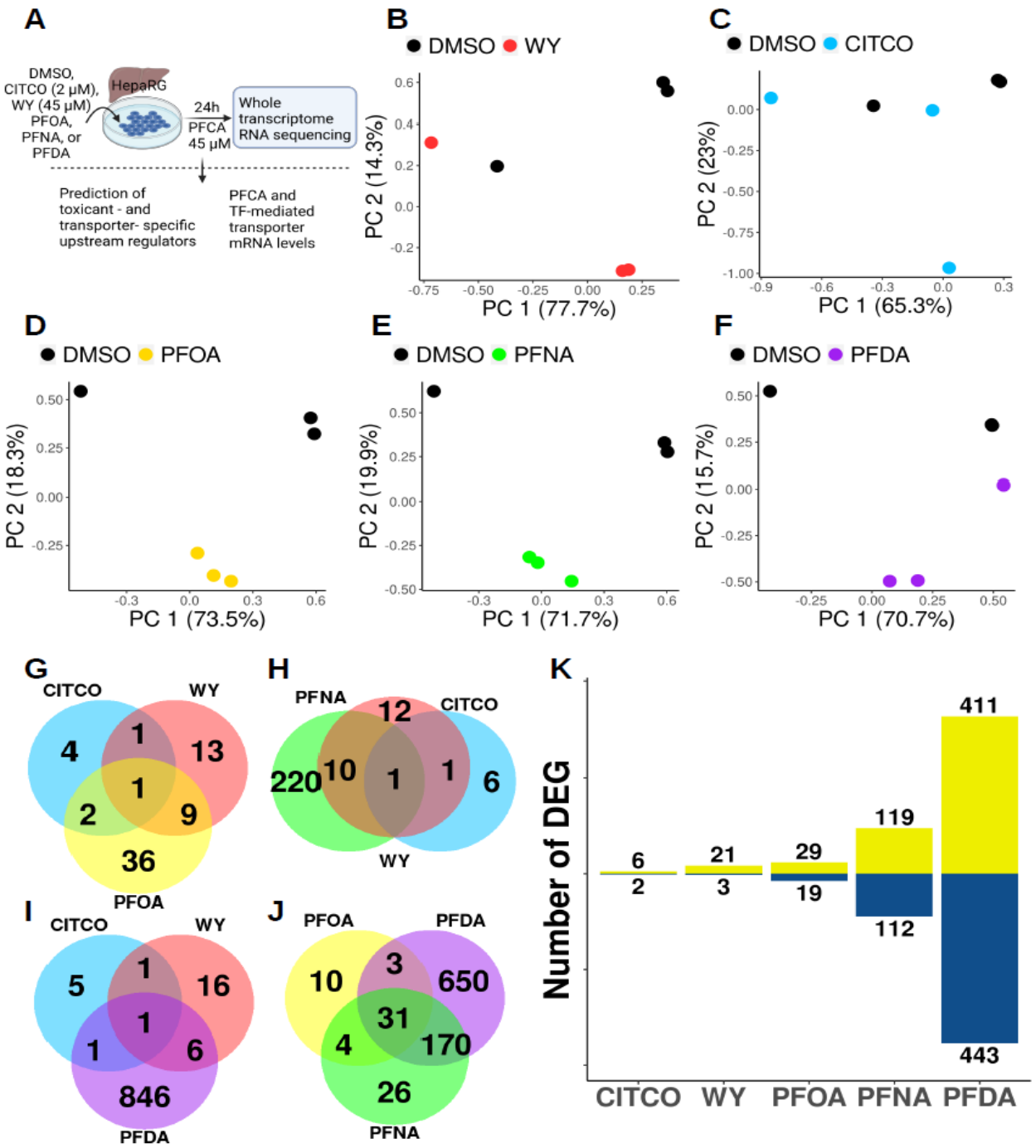

Figure 1. (A) Experimental design: HepaRG cells were exposed to 0.1% DMSO (vehicle control), 6-(4-chlorophenyl)imidazo[2,1-b][1,3]thiazole-5-carbaldehyde O-(3,4dichlorobenzyl)oxime (CITCO, constitutive androstane receptor ligand), WY-14643 (WY, peroxisome proliferator-activated receptor aligand), perfluorooctanoic acid (PFOA), perfluorooctanoic acid (PFNA), or perfluorodecanoic acid (PFDA). RNA was extracted and whole transcriptome RNA sequencing was conducted. The transcriptomic changes following each chemical exposure, as well as the predicted upstream regulators, were quantified. The mRNA levels in genes involved in liver functions, i.e., xenobiotic metabolism,

transporters, bile acid metabolism, amino acid metabolism, and carbohydrate metabolism were assessed. A specific focus of the present study was to assess the regulation of various xenobiotic and endobiotic transporters by perfluorinated carboxylic acids and their predicted upstream transcription factors. P CA results showing the first two principal components comparing DMSO to WY (B), CIT CO (C), P FOA (D), PFNA (E), and PFDA (F). G. Venn diagram comparing CITCO, WY, and PFOA. F. Venn diagram comparing CITCO, WY, and PFNA. H. Venn diagram comparing CITCO, WY, and PFDA. I. Venn diagram comparing PFOA, PFNA, and PFDA. K. Number of differentially regulated genes as defined by false discovery rate–Benjamini-Hochberg adjusted p-value < 0.05 and absolute fold change > 1.5 by each chemical.

Venn diagrams are used to visualize the commonly and differentially regulated genes following exposure to PFCAs, and how the PFCA effects compare to the effects of WY or CITCO (Fig. 1G-1J). For all the 3 PFCAs, most of the PFCA-regulated genes did not overlap with the WY- or CITCO-regulated genes. Within the commonly regulated genes between the nuclear receptor ligands and PFCAs, the transcriptomic signatures of PFCA exposure were more similar to that of WY exposure than CITCO exposure (Fig. 1G-1I), indicating that PPARα activation is a more prevalent mechanism in the transcriptional regulation of these genes than CAR activation. Common targets (31 genes) by all 3 PFCAs were also identified (Fig. 1J). These commonly regulated genes by all 3 PFCAs were involved in amino acid metabolism and carbon utilization (Fig. S2B and Table S3A). Among all 3 PFCAs, PFNA and PFDA had the greatest number of commonly regulated genes (170), with PFOA having the least number of overlapping differentially regulated genes (Fig. 1G). Commonly regulated genes by PFNA and PFDA were enriched in tRNA aminoacylation and carbohydrate metabolism (Fig. S2C and Table S3B). To assess the transcriptomic impact of PFCAs with varying carbon chain lengths, the number of differentially regulated genes was compared. Overall, the transcriptomic response was associated with carbon chain length of PFCAs with PFDA (C10) having the most prominent effect on the liver transcriptome (411 up-regulated genes and 433 down-regulated genes (Fig. 1K). This was followed by PFNA (119 up-regulated and 112 down-regulated genes) and PFOA

(29 up-regulated and 19 down-regulated genes) (Fig. 1K). In contrast, CITCO and WY produced minimal effect on the liver gene expression, in general (6 up-regulated and 2 down-regulated genes for CITCO, and 21 up-regulated and 3 down-regulated genes for WY) (Fig. 1K). In summary, most PFCA-mediated dysregulated genes were distinct from PPARα- and CAR-mediated pathways, whereas within the commonly regulated genes between PFCAs and the nuclear receptor ligands, the PPARα-signaling appears to be more involved than the CAR-signaling in PFCA-mediated transcriptomic response. All 3 PFCAs commonly regulated genes involved in amino acid synthesis and amino acid transport, whereas PFNA and PFDA also commonly regulated in tRNA activity and carbohydrate starvation. These results suggest that transporter-mediated protein synthesis and carbohydrate metabolism genes are critical targets in human hepatocytes following exposure to PFCAs.

Individual transcriptomic alterations following exposure to PFOA, PFNA, or PFDA

To compare the effect of the prototypical nuclear receptor ligands and different PFCAs on the hepatic transcriptome, differentially regulated genes were analyzed for each exposure group. As expected, CITCO up-regulated the CAR-target gene CYP2B6 (Supplemental Fig. 3A and Supplemental Table 4A). In addition, CYP1A2, and CYP3A4 were also upregulated by CITCO. Gene ontology enrichment results of differentially regulated genes included upregulation of epoxygenase P450 pathway and drug catabolic processes by CITCO (Supplemental Fig. 3B and Supplemental Table 4B). Also as expected, WY upregulated CYP4A22, a prototypical target of PPARα. Other genes up-regulated by WY include fibroblast

growth factor 21 (FGF21) – another known PPARα-target (Inagaki et al., 2007), as well as pyruvate dehydrogenase 4 (PDK4), fatty acid binding protein 4 (FABP4), and transmembrane protein 50B (TMEM50B) (Supplemental Fig. 3C and Supplemental Table 4C). At the pathway level, WY exposure up-regulated genes involved in multiple lipid metabolism-related pathways (Fig. S3D and Table S4D). No gene ontology terms were down-regulated by CITCO or WY.

PFOA up-regulated genes including ChaC glutathione specific gamma-glutamylcyclotransferase 1 (CHAC1), PDK4, CYP4A22, and down-regulated genes such as acireductone dioxygenase 1 (ADI1), neurobeachin pseudogene 2 (NBEAP2), and small EDRK-rich factor 1B (SERF1B) (Fig. 2A and Supplemental Table 5A). Upstream regulators from differentially regulated gene information include predicted activated transcription factors (TFs) involved in xenobiotic biotransformation (nuclear receptor subfamily 1 group I member 2 [NR1I2/PXR]), lipid sensing and metabolism (peroxisome proliferator activated receptor alpha and gamma [PPARα, PPARγ, respectively]), signaling molecule regulation (hepatocyte nuclear factor 4 alpha [HNF4α], activating transcription factor 4 [ATF4], forkhead box a2 [FOXA2]), and cell cycle regulation (RELA proto-oncogene [RELA], MYC proto-oncogene [MYC]), and predicted inhibited oxygen sensing (hypoxia inducible factor 1a [HIF1A]) (Supplemental Fig. 4A and Supplemental Table 5B). Up-regulated genes by PFOA were generally involved in transport processes such as carboxylic acid transport, organic acid transport, organic anion transport, and L-amino acid transport, as well as lipid metabolic process, as evidenced by the top enriched GO terms from the pathways analysis using TopGO; whereas no significant gene ontology terms were down-regulated by PFOA-exposure (Fig. 2B-2C, and Supplemental Table 5C).

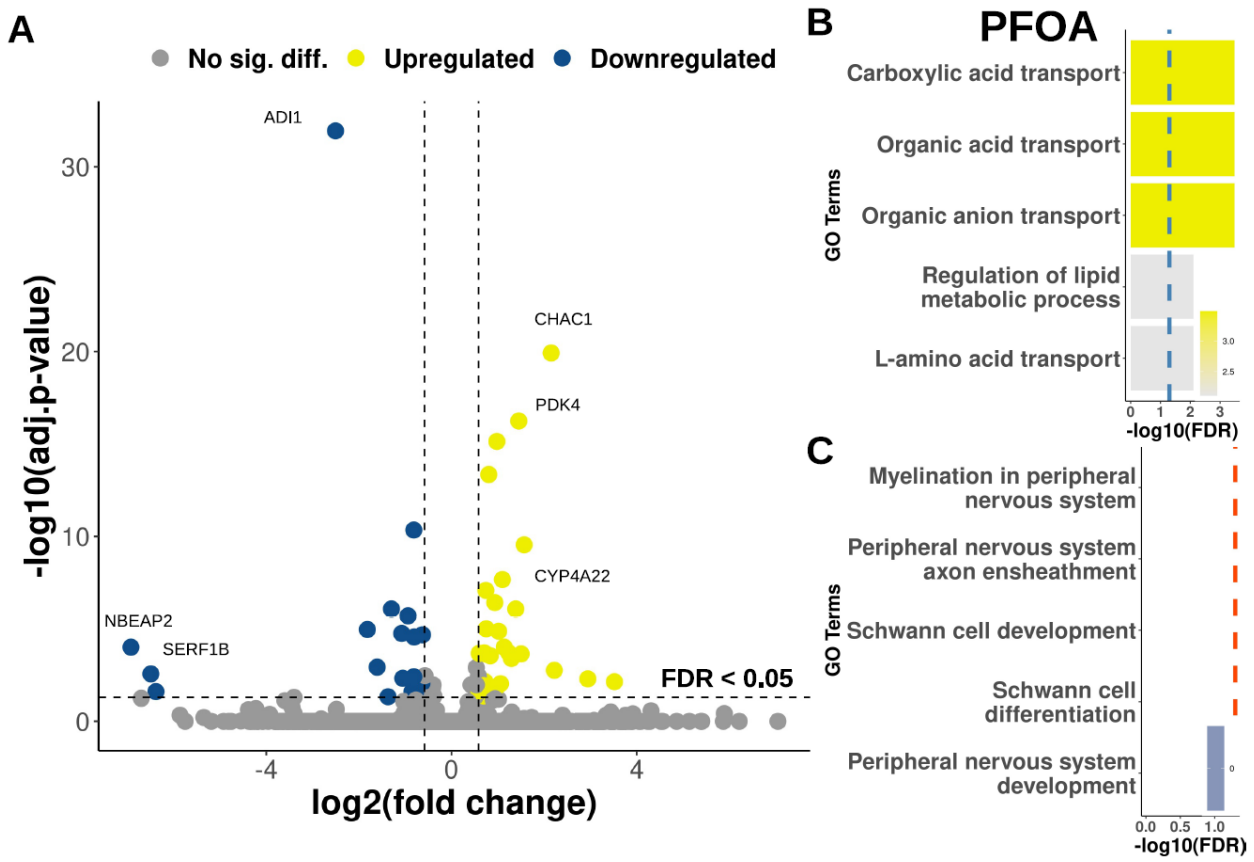

Figure 2. (A) Volcano plot showing differentially regulated genes by perfluorooctanoic acid relative to DMSO. Top 5 up- (B) and down- (C) regulated gene ontology terms from perfluorooctanoic acid. Color gradient represents false discovery rate-adjusted p-value. Vertical line shows statistical threshold (false discovery rate–Benjamini-Hochberg adjusted p-value < 0.05). Differentially regulated genes (false discovery rate–Benjamini-Hochberg adjusted p-value < 0.05 and absolute fold change > 1.5) were used for all plots.

Genes upregulated by PFNA include CHAC1, phosphoserine aminotransferase 1 (PSAT1), and FGF21, and down-regulated genes included chaperonin containing TCP1 subunit 8 pseudogene 1 (CCT8P1) (Fig. 3A and Supplemental Table 6A). As shown in Supplemental Table 6B, xenobiotic biotransformation regulators (aryl hydrocarbon receptor [AHR], NR1I2/PXR), lipid sensing and metabolism (PPARα), signaling molecule regulation (ATF4, estrogen receptor 1 [ESR1], progesterone receptor [PGR], forkhead box m1 [FOXM1]), cell cycle (RELA, specific protein 1 [SP1], SWI/SNF related matrix associated actin dependent

regulator of chromatin subfamily A member 4 [SMARCA4], transcription factor 3 [TCF3], CCAAT/enhancer binding protein alpha [CEBPA]), and immune response (nuclear factor kappa B subunit 1 [NFKB1]) were predicted to be activated. Transcription factors involved in lipid sensing and metabolism (PPARγ coactivator 1 alpha [PPARGC1A/PGC1α]) and oxygen sensing (hypoxia inducible factor 1 subunit alpha [HIF1α]) were predicted to be inhibited. Signaling molecule regulators (HNF4α and ATF5) and xenobiotic biotransformation regulator (nuclear receptor subfamily 1 group I member 3 [NR1I3/CAR]) were also predicted to be upstream regulators (Supplemental Fig. 4B). Up-regulated genes by PFNA were involved in tRNA aminoacylation, amino acid metabolism, as well as endoplasmic reticulum stress response (Fig. 3B and Supplemental Table 6C). Down-regulated genes by PFNA were related to changes in genes associated with the metabolism of alcohol groups, as well as cellular hypoxic response (Fig. 3C and Supplemental Table 6D).

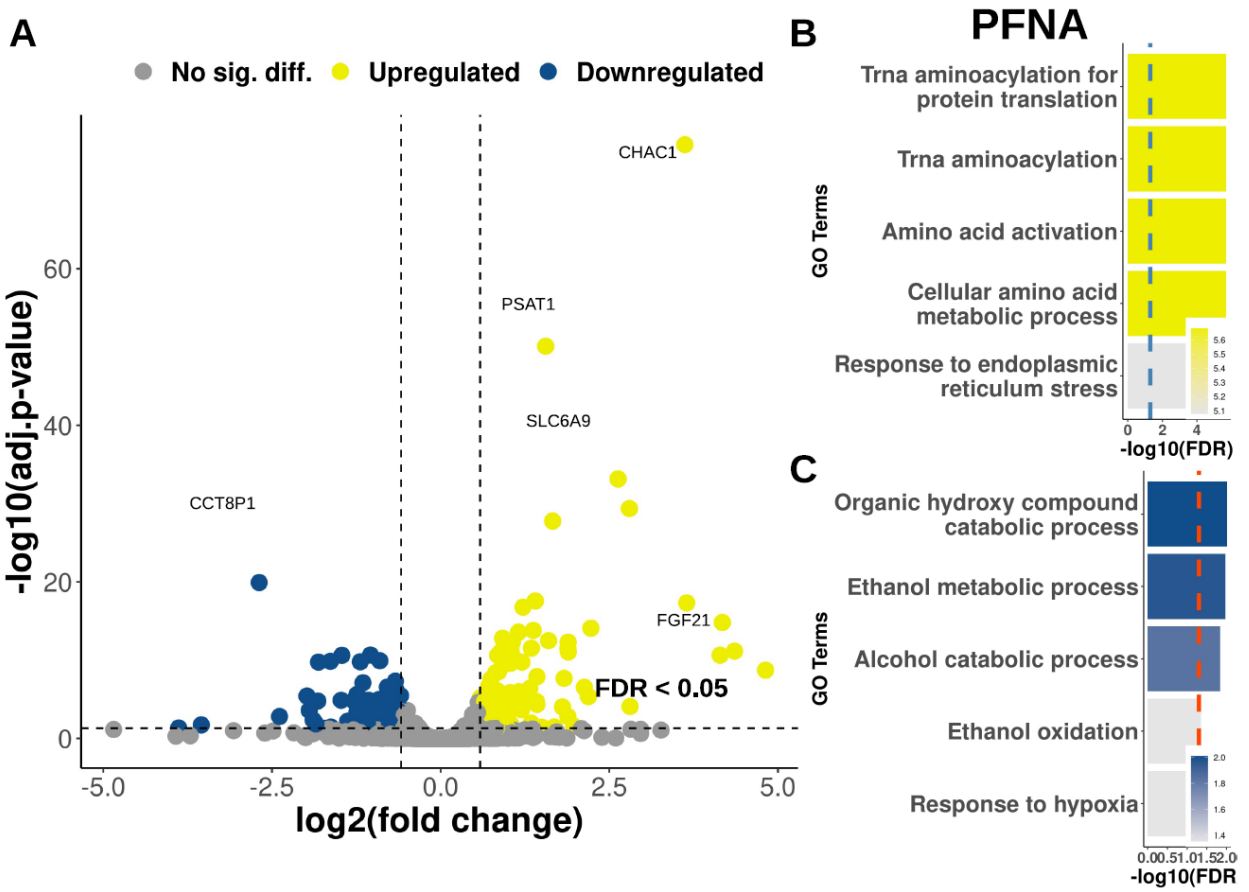

Figure 3. (A) Volcano plot showing differentially regulated genes by perfluorooctanoic acid relative to DMSO. Top 5 up- (B) and down- (C) regulated gene ontology terms from perfluorooctanoic acid. Color gradient represents false discovery rate-adjusted p-value. Vertical line shows statistical threshold (FDR-BH < 0.05). Differentially regulated genes (FDR-BH < 0.05 and absolute fold change > 1.5) were used for all plots.

PFDA-upregulated genes, such as CHAC1, PSAT1, bile acid-CoA amino acid N-acyltransferase (BAAT), and FGF21, as well as PFDA-downregulated genes including isopentyl-diphosphate delta isomerase 1 (IDI1), dehydrogenase/reductase 11 (DHRS11), and SERF1B are shown in Fig. 4A and Supplemental Table 7A. Activated predicted upstream regulators were involved in signaling molecule regulation (ATF4, SMAD family member 3 and 4 [SMAD3 and SMAD4, respectively], PGR, ESR1, homeobox b7 [HOXB7], NKX homeobox 1 [NKX3-1, androgen-regulated homeobox]), lipid sensing and metabolism (PPARγ and PPARα), xenobiotic

biotransformation (nuclear factor erythroid 2 like 2 [NFE2L2/NRF2]), oxygen sensing (hypoxia inducible factor 2 subunit alpha [HIF2A/EPAS1]), cell cycle (SMARCA4, histone deacetylase 2 [HDAC2], tumor protein 53 [TRP53], RNA binding motif protein X linked [RMBX], Fos proto-oncogene, AP1 transcription factor subunit [FOS], HIX ZBTB transcriptional repressor 1 [HIC1], kruppel like factor 6 [KLF6], Bon Hipel-Lindau tumor suppressor [VHL], enhancer of zeste 2 polycomb repressive complex 2 subunit [EZH2]), and ER stress (X-box binding protein 1 [XBP1]) (Supplemental Figure 4B and Supplemental Table 7B). Upstream regulators predicted to be inhibited consist of functions related to lipid sensing and metabolism (sterol regulatory element binding protein 1 and 2 [SREBF1 and SREBF1, respectively], PPARGC1A/PGC1a), bile acid metabolism (nuclear receptor subfamily 1 group h member 4 [NR1H4/FXR]), xenobiotic biotransformation (NR1I3/CAR), and signaling molecule regulation (HNF4α) (Supplemental Figure 4B and Supplemental Table 7B). Upstream transcription factors related to oxygen sensing (HIF1a), cell cycle (SP1), xenobiotic biotransformation (NR1I2/PXR), as well as lipid-sensing and metabolism (PPARD) were also predicted to be altered (Fig. S4C and Table S7B). Following PFDA exposure, the top 5 up-regulated gene ontology terms included cellular endoplasmic reticulum stress, tRNA aminoacylation, and amino acid metabolism (Fig. 4B and Supplemental Table 7C). Down-regulated genes were related to alcohol, sterol, and cholesterol metabolism, suggesting deviations from normal hepatic metabolic functions (Fig. 4C and Supplemental Table 7D).

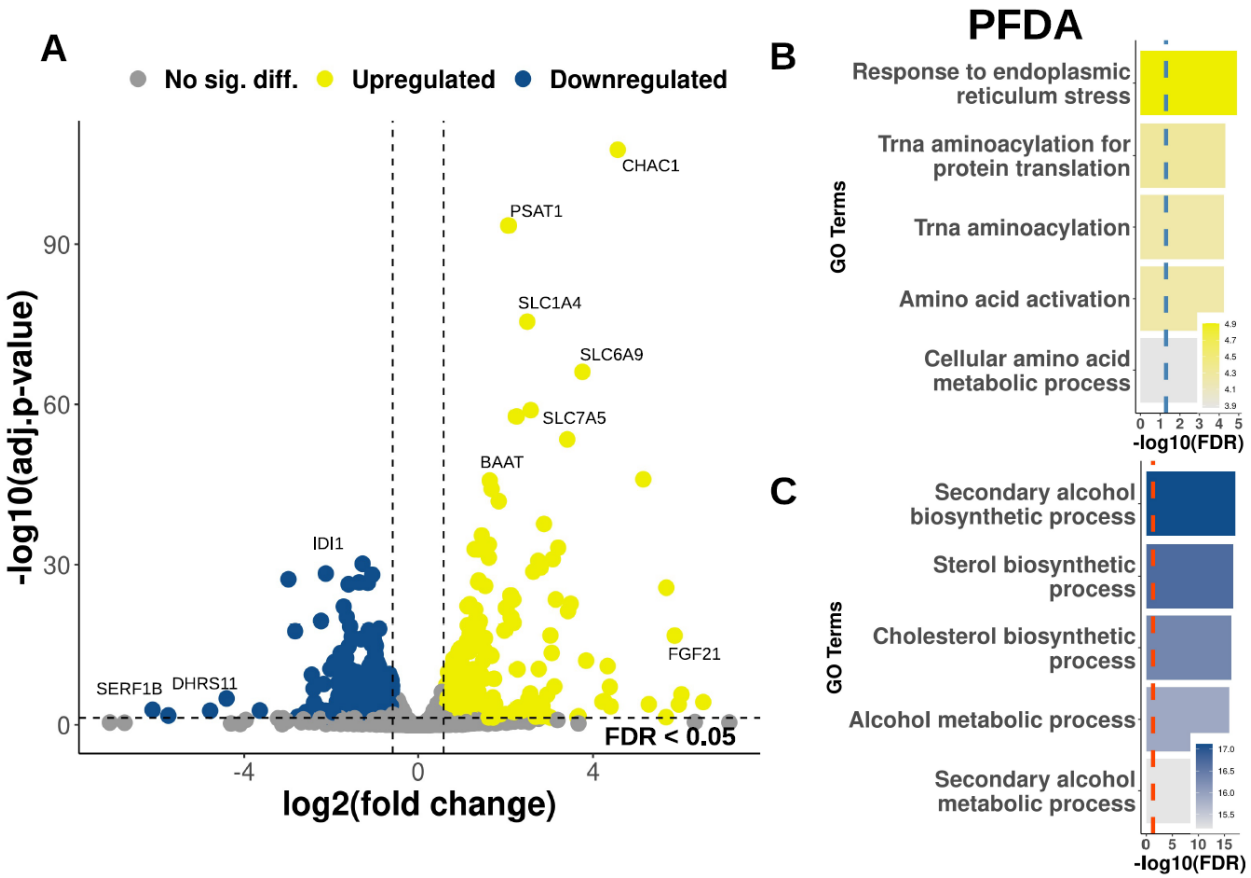

Figure 4. (A) Volcano plot showing differentially regulated genes by perfluorodecanoic acid relative to DMSO. Top 5 up- (B) and down- (C) regulated gene ontology terms from perfluorodecanoic acid. Color gradient represents false discovery rate-adjusted p-value. Vertical line shows statistical threshold (false discovery rate–Benjamini-Hochberg adjusted p-value < 0.05). Differentially regulated genes (false discovery rate–Benjamini-Hochberg adjusted p-value < 0.05 and absolute fold change > 1.5) were used for all plots.

Transcriptomic changes related to hepatic functions by PFCAs

Gene ontology enrichment of differentially regulated genes by PFCAs was suggestive of changes in endogenous liver functions, in addition to potential dysregulations in transporters (Figs 2-4). Therefore, to investigate the overall transcriptomic changes involved in endogenous liver functions and linked to the predicted upstream regulators, differentially regulated genes

were grouped into categories, namely phase-I and -II metabolism, transporters, bile acid metabolism, amino acid metabolism, and carbohydrate metabolism (Fig. 5 and Supplemental Fig. 4-5). In general, the numbers of differentially regulated genes increased with increasing carbon chain length of the PFCAs, whereas the overlap between the effect of PFCAs and the effect of CAR/PPARα ligands was minimal.

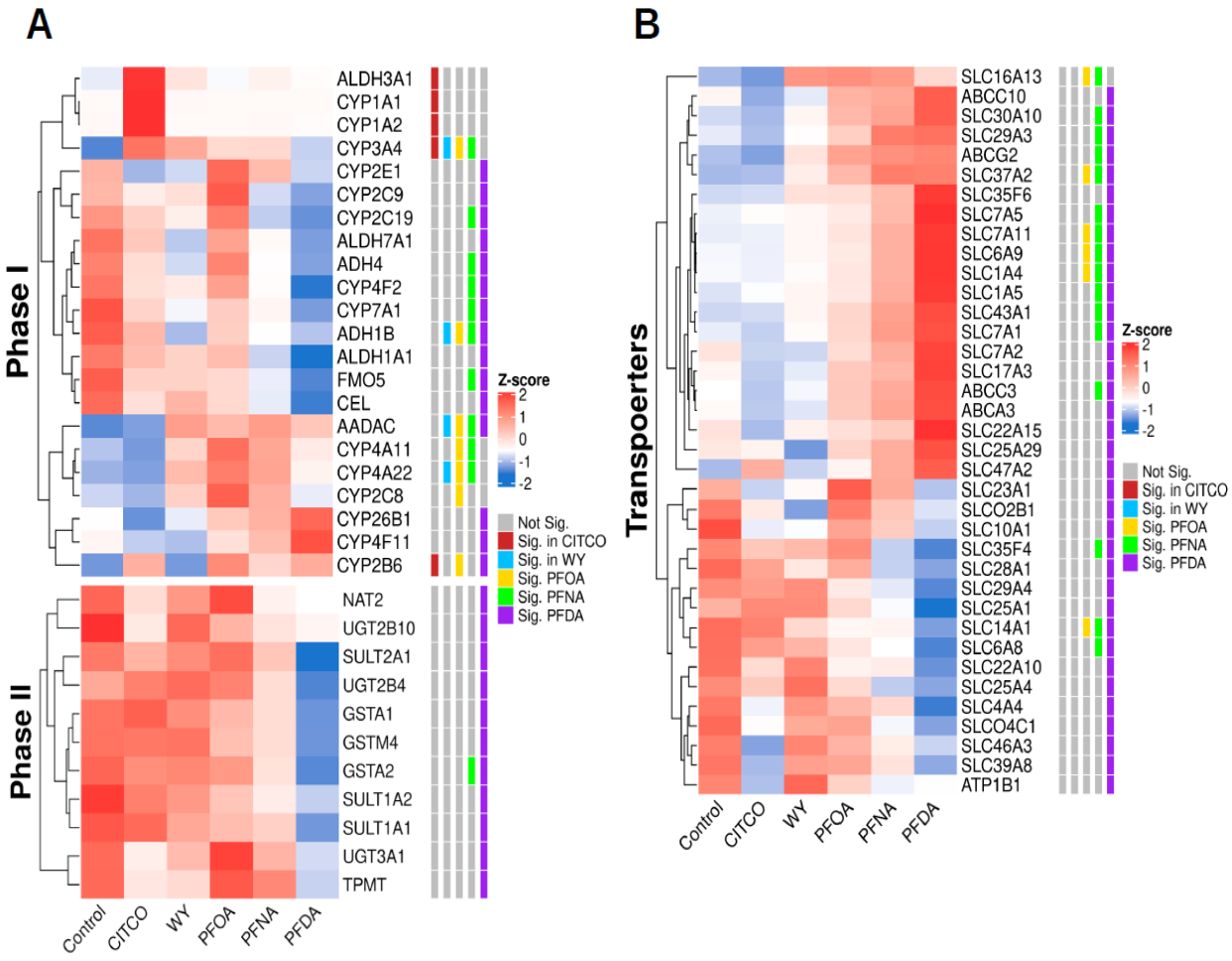

Figure 5. One-way hierarchical clustering of genes involved in phase-I and -II metabolism (A) and transporters (B) as regulated by 6-(4-chlorophenyl)imidazo[2,1-b][1,3]thiazole-5-carbaldehyde O-(3,4-dichlorobenzyl)oxime, WY-14643, perfluorooctanoic acid, perfluorooctanoic acid, and perfluorodecanoic acid. All differentially expressed genes at least by one exposure group were used for hierarchical clustering. Higher expression is shown in red and lower expression is represented in blue. All differentially expressed genes (false discovery rate–Benjamini-Hochberg adjusted p-value < 0.05) without fold-change threshold were categorized and used. Colored bars in heatmaps represent genes that are differentially regulated in a particular exposure group, i.e., 6-(4-chlorophenyl)imidazo[2,1-

b][1,3]thiazole-5-carbaldehyde O-(3,4-dichlorobenzyl)oxime–red, WY-14643–blue, perfluorooctanoic acid–yellow, perfluorooctanoic acid–green, perfluorodecanoic acid – purple.

Specifically, as shown in Fig. 5A and Supplemental Fig. 4D-4E, for phase-I and -II drug-metabolizing enzymes, the prototypical CAR ligand up-regulated 5 the mRNAs of 5 phase-I enzyme-endocing genes, namely *ALDH3A1*, *CYP1A1*, *CYP1A2*, *CYP3A4*, and *CYP2B6*. The up-regulation of *CYP1A2*, *CYP3A4*, and *CYP2B6* observed from the RNA-Seq experiment was consistent with the RT-qPCR results (Supplemental Fig. 1). The prototypical PPARα ligand WY up-regulated the phase-I enzymes *CYP3A4*, *ADH1B*, *AADAC*, and *CYP4A22*, and tended to up-regulate *CYP4A11* but was not statistically significant, and this trend was consistent with the RT-qPCR results (Supplemental Fig. 1). Neither CITCO nor WY altered the mRNAs of phase-II enzymes. Regarding the effects of various PFCAs on the mRNAs of phase-I drug-metabolizing enzymes, most of the PFOA effect was up-regulatory (e.g. *CYP3A4*, *AADAC*, *CYP4A11*, *CYP4A22*, *CYP2C8*, and *CYP2B6*). Conversely, most of the PFNA effect was down-regulatory (e.g. *CYP2C19*, *ADH4*, *CYP4F2*, *CYP7A1*, *ADH1B*, *FMO5*, *GSTA2*). PFDA had the most effect on the mRNAs of drug-metabolizing enzymes, and most of its effect was down-regulatory (e.g. *CYP2E1*, *CYP2CC9*, *CYP2C19*, *ALDH7A1*, *ADH4*, *CYP4F2*, *CYP7A1*, *ADH1B*, *ALDH1A1*, *FMO5*, *CEL*), as well as all the differentially regulated phase-II enzymes (Fig. 5A and Supplemental Fig. 4D-4E).

Regarding transporters, as shown in Fig. 5B and Supplemental Fig. 4C, neither CITCO nor WY altered the any transporter mRNAs, whereas PFCAs with increasing carbon chain length differentially regulated more transporter mRNAs, suggesting that PFCAs with longer carbon chains are more potent in regulating transporters, and the regulatory mechanisms are distinct from CAR and PPARα mediated pathways. Specifically, PFOA up-regulated five and down-

regulated one transporters, PFNA up-regulated ten and down-regulated three transporters, whereas PFDA up-regulated fourteen and down-regulated eleven transporters (Fig. 5B and S4F). The specific transporter regulatory patterns categorized according to their specific functions are shown in Fig. 6-10.

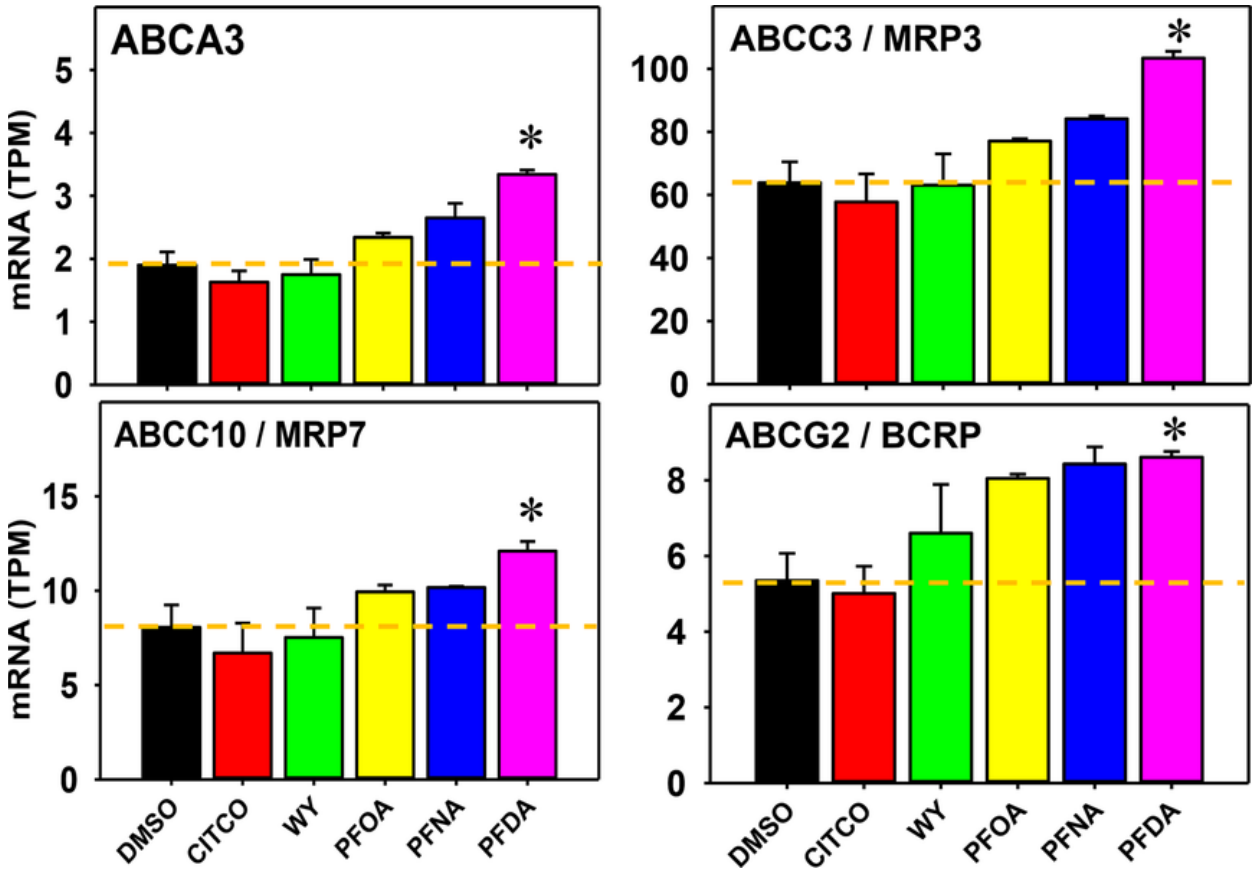

Figure 6. Bar plots showing the up-regulation of ABC transporters by 6-(4-chlorophenyl) imidazo[2,1-b] [1,3]thiazole-5-carbaldehyde O-(3,4-dichlorobenzyl)oxime, WY-14643, perfluorooctanoic acid, perfluorooctanoic acid, or perfluorodecanoic acid. Data are expressed as mean ± standard error (SE). Bar plots were made by using Sigma Plot (SPSS, Inc., Chicago, IL). Asterisks represent statistically significant differences as compared with the 0.1% DMSO-exposed vehicle group (DESeq2, false discovery rate– Benjamini-Hochberg adjusted p-value < 0.05).

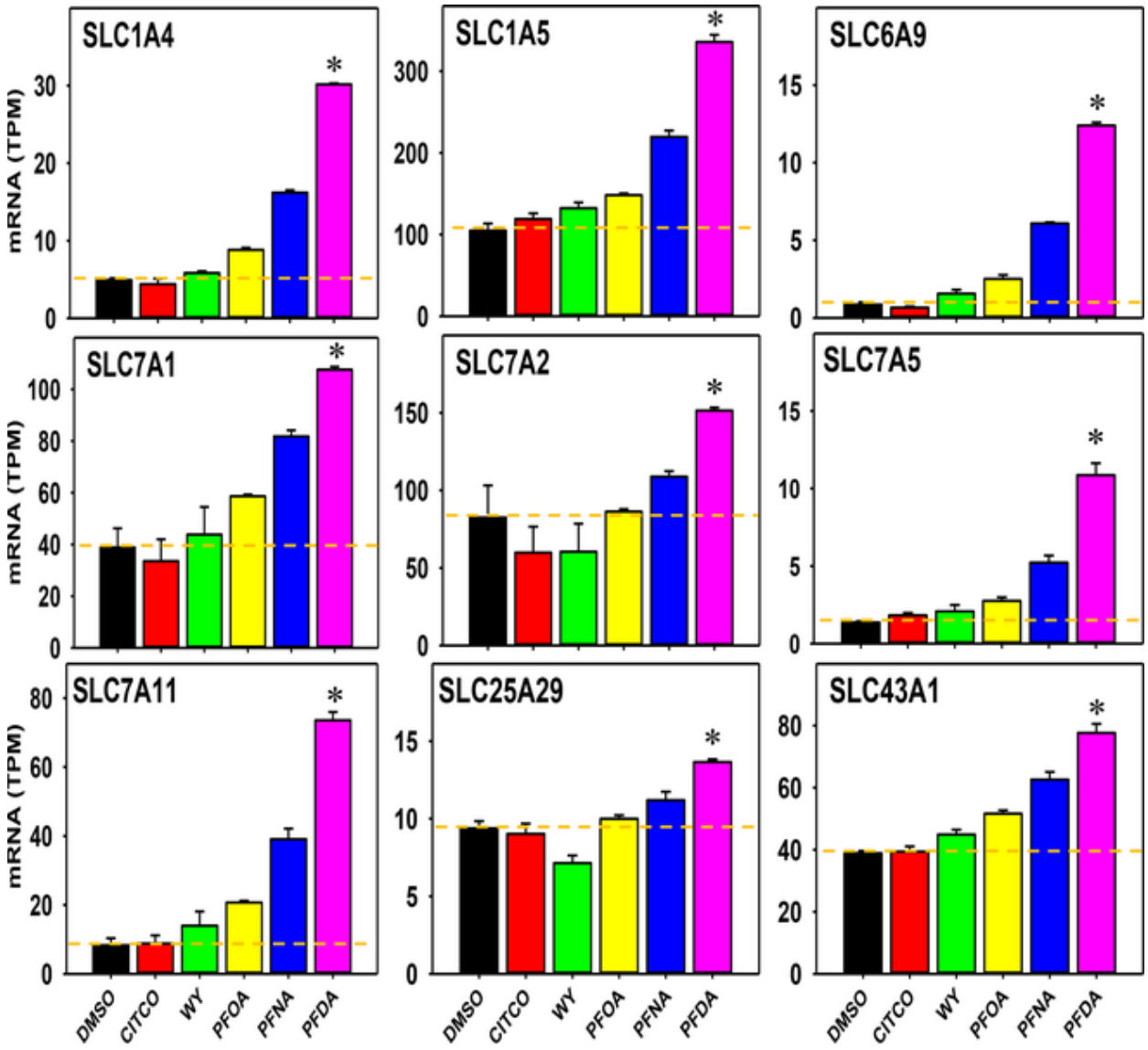

Figure 7. Bar plots showing the up-regulation of amino acids transporters by 6-(4-chlorophenyl)imidazo[2,1-b] [1,3]thiazole-5-carbaldehyde O-(3,4-dichlorobenzyl)oxime, WY-14643, perfluorooctanoic acid, perfluorooctanoic acid, or perfluorodecanoic acid. Data are expressed as mean ± standard error (SE). Bar plots were made by using Sigma Plot (SPSS, Inc., Chicago, IL). Asterisks represent statistically significant differences as compared with the 0.1% DMSO-exposed vehicle group (DESeq2, false discovery rate– Benjamini-Hochberg adjusted p-value < 0.05).

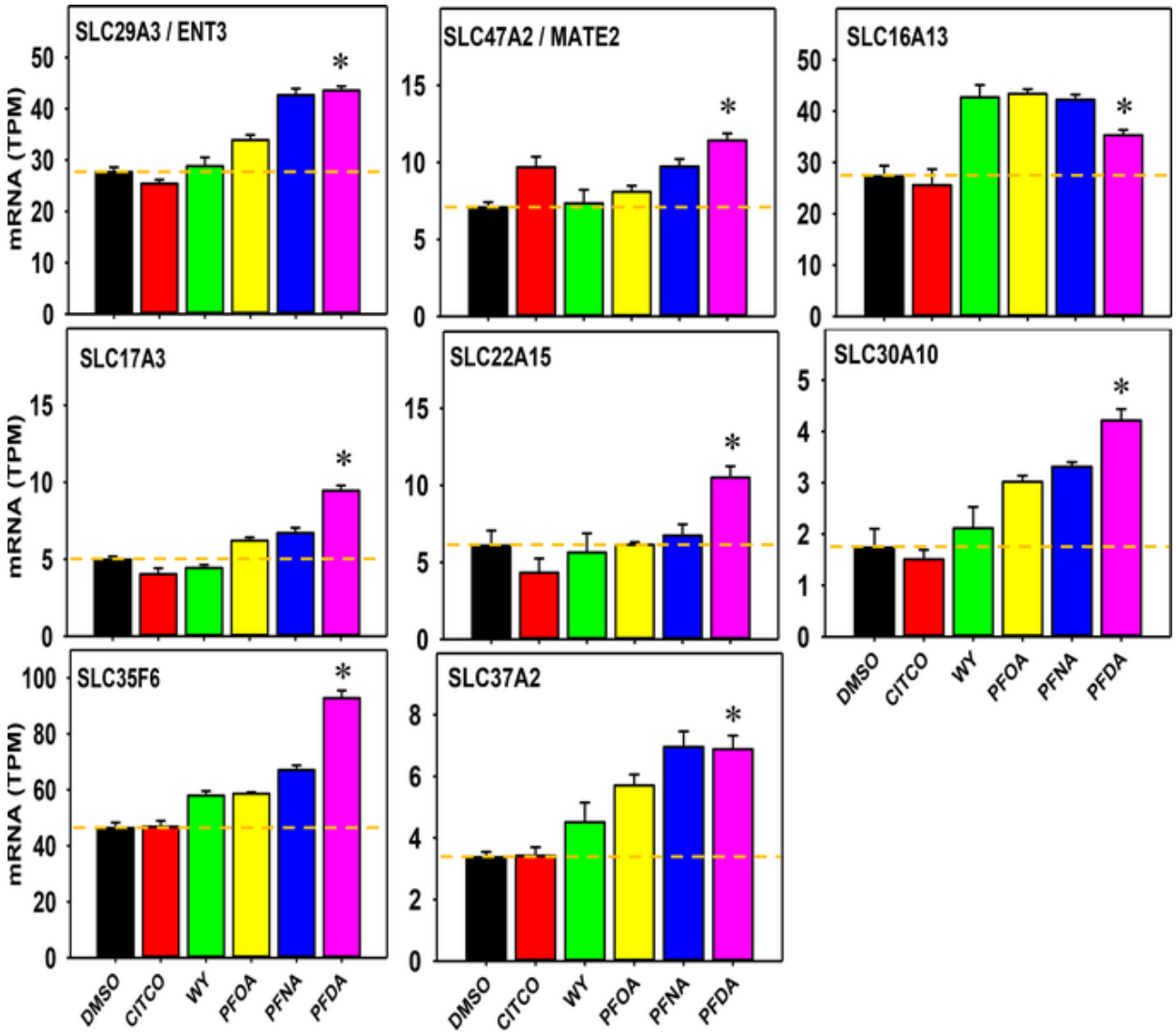

Figure 8. Bar plots showing the up-regulation of other SLC transporters by 6-(-4-chlorophenyl)imidazo[2,1-b] [1,3]thiazole-5-carbaldehyde O-(3,4-dichlorobenzyl)oxime, WY-14643, perfluorooctanoic acid, perfluorooctanoic acid, or perfluorodecanoic acid. Data are expressed as mean ± standard error (SE). Bar plots were made by using Sigma Plot (SPSS, Inc., Chicago, IL). Asterisks represent statistically significant differences as compared with the 0.1% DMSO-exposed vehicle group (DESeq2, false discovery rate– Benjamini-Hochberg adjusted p-value < 0.05).

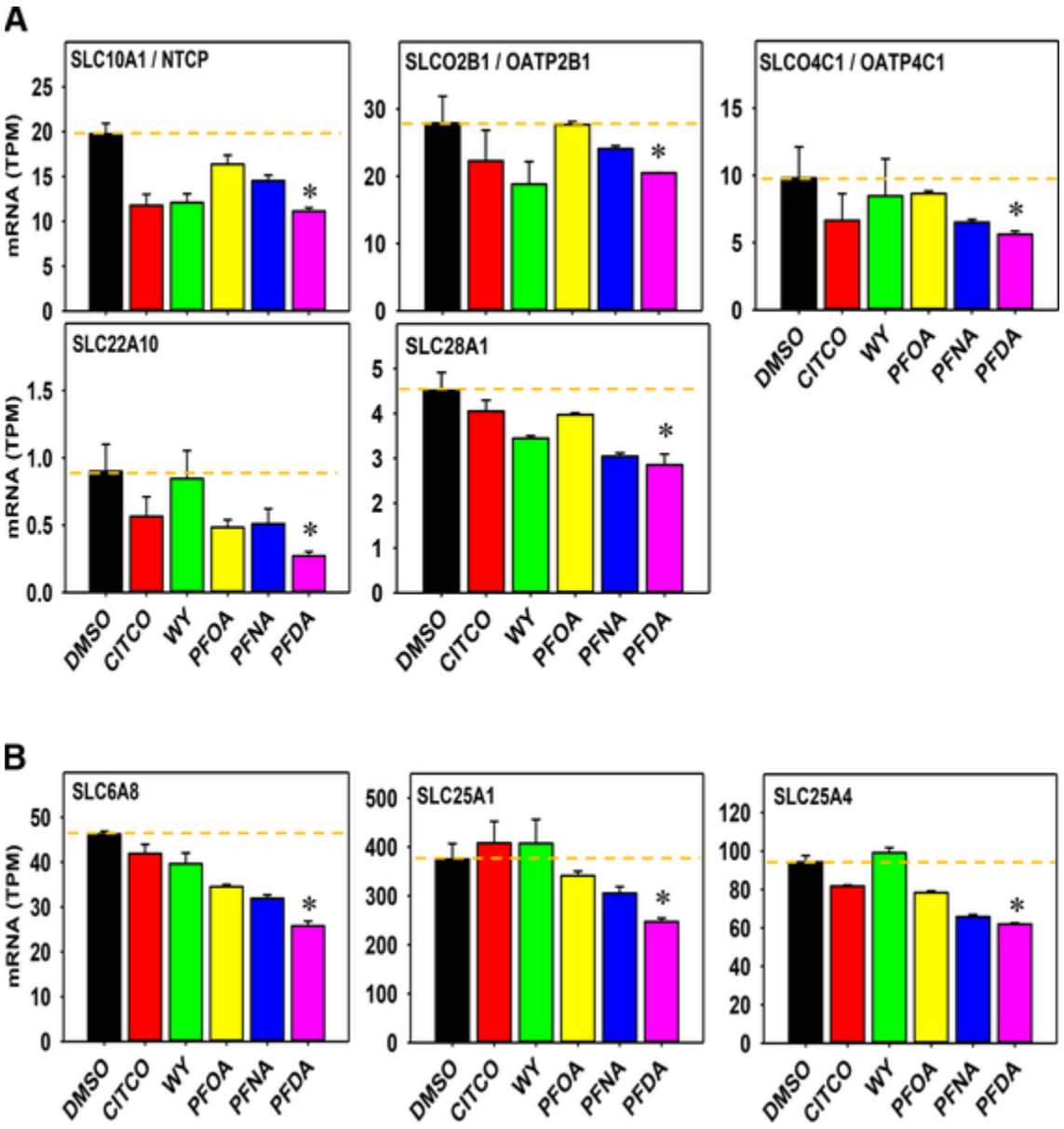

Figure 9. Bar plots showing the down-regulation of SLC transporters by 6-(4-chlorophenyl)imidazo[2,1-b] [1,3]thiazole-5-carbaldehyde O-(3,4-dichlorobenzyl)oxime, WY-14643, perfluorooctanoic acid, perfluorooctanoic acid, or perfluorodecanoic acid. Data are expressed as mean ± standard error (SE). Bar plots were made by using Sigma Plot (SP SS, Inc., Chicago, IL). Asterisks represent statistically significant differences as compared with the 0.1% DMSO-exposed vehicle group (DESeq2, false discovery rate– Benjamini-Hochberg adjusted p-value < 0.05).

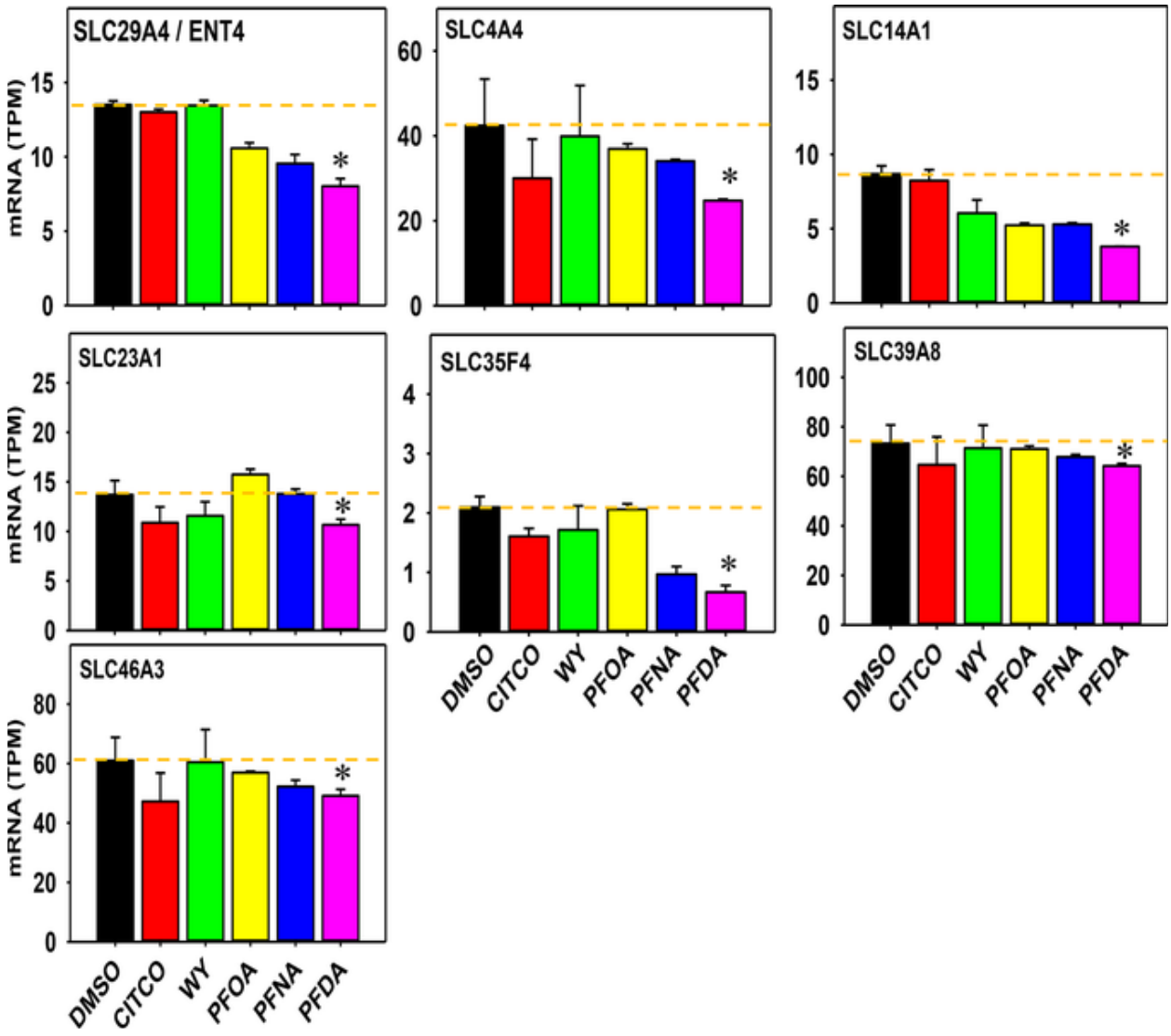

Figure 10. Bar plots showing the down-regulation of other SLC transporters by 6-(4-chlorophenyl)imidazo[2,1-b][1,3]thiazole-5-carbaldehyde O-(3,4-dichlorobenzyl)oxime, WY 14643, perfluorooctanoic acid, perfluorooctanoic acid, or perfluorodecanoic acid. Data are expressed as mean ± standard error (SE). Bar plots were made by using Sigma Plot (SP SS, Inc., Chicago, IL). Asterisks represent statistically significant differences as compared with the 0.1% DMSO-exposed vehicle group (DESeq2, false discovery rate–Benjamini-Hochberg adjusted p-value < 0.05).

Bile acid metabolism-related genes were not regulated by CITCO, WY, or PFOA, and most of the PFNA- and PFDA-mediated mRNA changes were down-regulatory. Specifically, PFNA decreased the mRNAs of *CYP7A1* (rate-limiting enzyme for BA-synthesis), as well as *DIO1*, *DIO2*, and *IDI1*; PFDA down-regulated most of the differentially regulated genes involved in BA metabolism (Supplemental Fig. 4G and 5A top panel).

Most genes related to amino acid metabolism were not regulated by CITCO or WY, except for a moderate mRNA increase of *PSAT1* by WY. The PFCA effect was partitioned into two clusters (Supplemental Fig. 5A bottom panel): genes in cluster 1 were up-regulated by PFCAs and genes in cluster 2 were down-regulated by PFCAs. For both clusters, the effect was more prominent with increasing carbon chain lengths of the PFCAs. Specifically, PFOA up-regulated two genes and down-regulated one genes; PFNA up-regulated sixteen and down-regulated two genes; PFDA up-regulated twenty-one genes and down-regulated twelve genes (Fig. S4H). As shown in Supplemental Fig. 5A, PFOA up-regulated genes related to amino acid biosynthesis (e.g. *YARS1*, *AARS*, *PSAT1*, *GPT2*, *ADI1*, and *MCCC1*), and down-regulated genes involved in methionine metabolism (e.g. *GNMT*) and mitochondrial permeability (e.g. *PPM1K*). PFNA up-regulated a greater number of genes involved in amino acid metabolism, compared to PFOA, such as asparagine and serine metabolism, and tRNA aminoacylation (e.g. *ATF4*, *YARS1*, *PHGDH*, *AARS1*, *PSAT1*, *PSPH*, *EPRS1*, *IARS1*, *TARS1*, *MARS1*, *SARS1*, *GARS1*, *WARS1*, *ASNS*) and down-regulated alpha amino acid metabolism (*HIBCH*, *ARG1*, *MCCC1*, and *ADSS1*). PFDA up-regulated all genes in the first cluster, which are involved in asparagine, serine, taurine, and glutamine metabolism, as well as carbon-nitrogen and tRNA aminoacyl activity (*ARG2*, *CARS1*, *ATF4*, *YARS1*, *PHGDH*, *AARS1*, *PSAT1*, *GPT2*, *PSPH*, *EPRS1*, *IARS1*, *TARS1*,

MARS1, *SARS1*, *GARS1*, *SLC7A11*, *WARS1*, *ASNS*, *GCLM*, *CTH*, *PHYKPL*, *GFPT1*, *CAD*, *PFAS*, *BAAT*) and most genes in the second cluster, most of which were related to branched chain and alpha amino acid catabolism, and S-adenosyl methionine binding (*HIBCH*, *PLOD2*, *ALDH1A1*, *ARG1*, *CDO1*, *ACAT1*, *HGD*, *UPB1*, *DIO1*, *GNMT*, *GPT*, *MCCC1*, *PPM1K*, *OTC*, *ABAT*, *GLYAT*, *ALDH7A1*, *HNF4A*, *CPS1*, *CBS*, *ADSS1*, *ACMSD*, *OGDH*, *SLC39A8*).

Genes involved in carbohydrate metabolism were not changed by CITCO. *PDK4* (involved in pyruvate metabolism) was upregulated by WY (Supplemental Fig. 5B). Carbohydrate metabolism-related genes were also grouped into two clusters showing down-regulated and up-regulated patterns, respectively (Supplemental Fig. 5B). PFOA up-regulated two genes and down-regulated two genes; PFNA up-regulated eight genes and down-regulated seven genes; PFDA up-regulated twenty-one genes and down-regulated twenty-four genes (Supplemental Fig. 4I). Specifically, as shown in Supplemental Figure 5B, PFOA up-regulated hexose metabolism-related genes (*FUT1*, *PDK4*, and *CPT1A*), and down-regulated *PFKFB4* and *ENO2*. The number of dysregulated genes increased, compared to PFOA. PFNA up-regulated genes related to metabolism of hexose and other carbohydrates, as well as glucagon signaling (e.g. *CHST3*, *ATF4*, *PCK2*, *FUT1*, *PYGB*, *B4GALT5*, *AMY2B*, *PDK4*, and *CPT1A*; and down-regulated *OMA1*, *ALDOB*, *ALDOC*, *LDHA*, *CHIA*, *INPP5J*, *PFKFB4*, and *ENO2*). PFDA dysregulated the most number of genes in the carbohydrate metabolism category. PFDA up-regulated genes involved in glucose and hexose metabolism, and regulation of gluconeogenesis (e.g. *HKDC1*, *OGT*, *IRS2*, *FOXK2*, *ATF4*, *PER2*, *PMAIP1*, *NUPR1*, *DDIT4*, *KCNJ11*, *SESN2*, *PCK2*, *FUT1*, *ATF3*, *SIK1*, *FOXK1*, and *PDK4*). PFDA down-regulated genes involved in canonical glycolysis and metabolism of NAD, pyruvate, and energy-related metabolites (e.g.,

ALDOB, glycerol-3-phosphate dehydrogenase 1, glucosylceramidase beta 3, phosphoenolpyruvate carboxykinase 1, myogenesis regulating glycosidase, phosphofructokinase, fructose-biphosphate A, citrate synthase, oxoglutarate dehydrogenase, pyruvate dehydrogenase E1 subunit alpha 1, malate dehydrogenase 1, glucose-6-phosphate isomerase, triosephosphate isomerase 1, IDH2, pyruvate kinase M1/2, phosphoglycerate kinase 1, ALDOC, hyaluronidase 1, lactate dehydrogenase A, chitinase acidic , phosphoglycerate mutase 1, PFKFB4, ENO2, aldehyde dehydrogenase 1 family member A1, GNMT, and glycogen synthase 1).

As a primary focus of the present study, we examined the effect of PFCAs on various families of transporters in HepaRG cells. Because an advantage of RNA-Seq over other conventional mRNA quantification methods is that it provides a "true measurement" of the actual transcript counts, allowing the comparison of the absolute abundance among different transporter genes, after we unveiled the relative expression patterns of transporters in a heatmap (Fig. 5), we compared the absolute transcript counts and regulation of these transporters under basal and PFCA-exposed conditions (Fig. 6-10 and Supplemental Fig. 7-10).

ABC transporters are the largest family of the transport ATPases (Supplemental Table 1) and they are involved in the efflux of various xenobiotics and endogenous metabolites. As shown in Supplemental Fig. 7, under basal conditions, among all the ABC transporters, the cumulative mRNAs of the ABCC sub-family were the most abundant (27%), followed by ABCB (19%), ABCA (17%), ABCD (16%), ABCE (10%), ABCF (9%), and ABCG (2%). Because ABCC/MRP and ABCB/MDR are the most important efflux transporters for various drugs, and ABCA is important for eliminating cholesterol and oxysterols, the highest abundance of the mRNAs of these two sub-families highlight the importance of hepatocytes in these two

functions. As shown in Fig. 6, following chemical exposure, CITCO and WY had no effect on the mRNAs of the ABC transporters. However, PFCAs with increasing carbon chain lengths tended to increase the mRNAs of ABCA3, ABCC3/MRP3, ABCC10/MRP7, and ABCG2/BCRP, with the statistical significance observed for PFDA. The up regulation of these ABC transporters may suggest a compensatory response to eliminate the intracellular toxic metabolites following PFCA exposure.

Besides the ABC transporters, the mRNAs of other transport ATPases were also detected in HepaRG cells, with ATP5 being the most abundant transport ATPase family (74.9%), followed by ATP6 (12.9%), ATP1 (8.4%), ATP2 (2.6%), and ATP13 (1.8%). Other transport ATPases had minimal expression in HepaRG cells (< 1%) (Supplemental Fig. 8). None of these transport ATPases were readily upregulated by the nuclear receptor ligands or PFCAs.

Another major transporter superfamily in humans is the solute carriers (SLCs), which play important roles in transporting endogenous metabolites, nutrients, and drugs. Within the SLC superfamily, the SLCO/OATP transporters are well-known for their uptake of various drugs and other xenobiotics into hepatocytes for further metabolism. As shown in Supplemental Fig. 9, under basal conditions, among all the OATP transporters, the cumulative mRNAs of the SLCO2/OATP2 sub-family were the most abundant (49%), followed by SLCO4/OATP4 (28%), SLCO3/OATP3 (13%), SLCO1/OATP1 (9%), SLCO5/OATP5 (1%), and SLCO6/OATP6 (0.03%). The cumulative mRNA of all SLCO/OATP transporters comprise approximately 0.2% of the mRNA abundance of all SLC transporters (Supplemental Fig. 10). The SLC transporter genes with highest expressed in HepaRG cells are those involved in amino acid transport, which is essential for protein synthesis (44%), followed by those involved in the transport of zinc

(8.0%) and iron (2.0%), as well as other nutrients such as folate, thiamine, and riboflavin (1.7%). While most of the HepaRG cell-expressed SLC transporter genes are involved in intermediary metabolism, a minor percentage of the SLC transporter genes expressed in HepaRG cells are involved in the transport of xenobiotics (ENTs [0.63%], OCTs/OCTNs [0.5%], MATEs [0.2%], and CNTs [0.05%]) and BAs (0.3%) (Fig. S10).

The PFCA-mediated gene regulation of amino acid transporting SLC transporters – the most abundant SLC members in HepaRG cells, is shown in Fig. 7. Interestingly, while the CAR and PPARα ligands had no effect, PFCAs within increasing carbon chain lengths tended to up-regulate genes for 9 SLC amino acid transporters, namely SLC1A4, SLC1A5, SLC6A9, SLC7A1, SLC7A2, SLC7A5, SLC7A11, SLC25A29, and SLC43A1, with statistical significance observed for PFDA. Similarly, other SLC transporters that tended to be up-regulated by PFCAs include those involved in xenobiotic transport (SLC29A3/ENT3 and SLC47A2/MATE2) with statistical significance observed for PFDA (Fig. 8). PFDA also upregulated genes for several SLC transporters for endogenous substrates, including the monocarboxylic acid transporter SLC16A3, the sodium phosphate transporter SLC17A3, the versatile cellular metabolite transporter SLC22A15, the manganese transporter SLC30A10, SLC35F6 (suggested to be a nucleotide-sugar transporter), and the glycerol-3-phosphate transporter SLC37A2 (GeneCards.org) (Fig. 8).

While most of the up-regulated genes for SLC transporters by PFDA are involved in intermediary metabolism including protein synthesis, the SLC transporters down-regulated by PFCAs include the major hepatic BA uptake transporter SLC10A1/NTCP, two OATP uptake transporters for xenobiotics (SLCO2B1 and SLCO4C1), as well as the organic anion/cation

transporter SLC22A10 and the sodium-coupled nucleoside transporter SLC28A1 (Fig. 9A). PFDA also downregulated genes for the creatine efflux transporter SLC6A8, the mitochondrial transporters SLC25A1 and SLC25A4 for citrate and adenine nucleotide (GeneCards.org) (Fig. 9B), the sodium bicarbonate cotransporter SLC4A4, the urea transporter SLC14A1, the ascorbic transporter SLC23A1, the equilibrative nucleoside transporter SLC29A4/ENT4, SLC35F4 (unknown function), the zinc transporter SLC39A8, and the lysosomal drug transporter SLC46A3 (Fig. 10).

Upstream regulators for PFCA-mediated regulation of transporters were predicted (Fig. S6). NFE2L2/NRF2, which is the major sensor for oxidative stress and electrophiles, was predicted to be the main upstream regulator for transporters regulated by all PFCAs (Fig. S6A). In addition, upstream factors predicted to be involved in PFNA-mediated transporter regulation include regulators involved in xenobiotic biotransformation (AHR, retinoic acid receptor a [RARα], retinoic X receptor a [RARα]), cell cycle (SMARCA4, SP1, signaling molecule regulation (msh homeobox 2 [MSX2], EPAS, splicing factor 1 (SF1), SRY box transcription factor 2 [SOX2], nuclear receptor subfamily 5 group A member 1 (NR5A1), PGR, ESR1, TWIST), and lipid sensing and metabolism (PPARγ) (Fig. S6B). Most of these upstream regulators were also predicted to be involved in PFDA-mediated transporter regulations (PGR, MSX2, SMARCA4, SP1, EPAS1, SF1, RXRα, AHR, SOX2, NR5A1, TWIST1, RARα). In addition, PFDA-mediated transporter regulation also appeared to involve nuclear receptor subfamily 3 group C member 2 [NR3C2/glucocorticoid receptor [GR]], the major bile acid receptor NR1H4/FXR, nuclear receptor subfamily 3 group C member 1 [NR3C1/ mineralocorticoid receptor], nuclear respiratory factor 1 [NRF1], HNF1a, the estrogen receptor 1

(ESR1), Spalt Like Transcription Factor 1 (SALL1), and NK2 Homeobox 1 (NKX2-1) (Fig. S6C).

Observations from CAR-null and Nrf2-null mice showed that Nr1I3/CAR and Nfe2l2/Nrf2 receptors are involved in the PFNA and PFDA mediated regulation of certain drug transporters in liver, respectively (Maher et al., 2008; Zhang et al., 2018) (Maher et al., 2008; Zhang et al., 2018) (Table 2). Interestingly, NRI13/CAR was also a predicted upstream regulator in PFNA-exposed HepaRG cells (Fig. 3B), and NFE2L2/NRF2 was also a predicted upstream regulator in PFDA-exposed HepaRG cells (Fig. 4B). Therefore, our findings from HepaRG cells align with the literature reports on PFNA- and PFDA-exposed mouse models. AHR is another important xenobiotic-sensing receptor, and it was only predicted to be activated by PFNA. The effect of PFNA on hepatic transporters is not characterized in AhR-null mice; the effect of PFOA of hepatic transporters is also not characterized in the receptor gene null mice discussed above. However, it is possible that some of the same xenobiotic-sensing receptors are also involved.

Table 1. PFCA-mediated regulation of transporters in HepaRG cells
(Italicized & underlined: present study; **bold**: similar trend of regulation between the present study and the literature)

PFCAs	Exposure time & concentration	Transporters	Effect
PFOA	48 h: 250 μM	ABCA1	↓ (Behr et al., 2020)
	24 h: 250 & 500 μM 48 h: 50, 100, & 250 μM	ABCB11/BSEP	
	24 h: 250 & 500 μM	ABCC2/MRP2	
	24 h: 500 μM 48 h: 10 & 50 μM	ABCC3/MRP3	
	24 h: 500 μM 45 h: 250 μM	ABCG1	
	24 h: 10, 50, 250, & 500 μM	ABCG5	

	48 h: 10, 50, 100, & 250 μM		
	24 h: 10, 50, 250, & 500 μM 48 h: 10, 50, & 250 μM	ABCG8	
	24 h: 10, 50, 250, & 500 μM 48 h: 100 & 250 μM	SLC10A1/NTCP	
	24 h: 250 & 500 μM 48 h: 100 & 250 μM	SLCO1B1/OATP1B1	
	24 h: 50, 100, & 250 μM 48 h: 10 & 50 μM	SLC51B/OSTβ	↑ (Behr et al., 2020)
	24 h: 100 μM	**SLC1A4**, SLC1A5, SLC3A2, SLC7A1, SLC7A2, SLC7A5, **SLC7A11**, SLC16A13, SLC27A2, **SLC37A2**, SLC43A1	↑ (Louisse et al., 2020)
		SLC2A2, SLC38A1, SLC38A3	↓ (Louisse et al., 2020)
	24 h: 45 μM	***SLC1A4,*** *SLC6A9,* ***SLC7A11****, SLC16A3,* ***SLC37A2***	↑ *Fig. 7*
		SLC14A1	↓ *Fig. 10*
PFNA	24 h: 100 μM	**SLC1A4, SLC1A5**, SLC3A2, **SLC7A1**, SLC7A2, **SLC7A5**, **SLC7A11**, **SLC16A13**, SLC27A2, **SLC37A2**, **SLC43A1**	↑ (Louisse et al., 2020)
		SLC2A2, SLC38A1, SLC38A3	↓ (Louisse et al., 2020)
	24 h: 45 μM	*ABCC3/MRP3, ABCG2/BCRP,* ***SLC1A4****,* ***SLC1A5****, SLC6A9,* ***SLC7A1, SLC7A5****,* ***SLC7A11****,* ***SLC16A13****, SLC29A3/ENT3, SLC30A10,* ***SLC37A2****,* ***SLC43A1***	↑ *Fig. 6*
		SLC6A8, SLC14A1, SLC35F4	↓ *Fig. 9B, 10*
PFDA	*24 h: 45 μM*	*ABCA3, ABCC3/MRP3, ABCC10/MRP10, ABCG2/BCRP, SLC1A4, SLC1A5, SLC6A9, SLC7A1, SLC7A2, SLC7A5, SLC7A11, SLC17A3, SLC22A15, SLC25A29, SLC29A3/ENT3, SLC30A10, SLC35F6, SLC37A2, SLC43A1, SLC47A2/MATE2*	↑ *Fig. 5B*
		ATP1B1, SLCO2B1/OATP2B1, SLCO4C1/OATP4C1, SLC10A1/NTCP, SLC4A4,	↓ *Fig. 5B*

		SLC6A8, SLC14A1, SLC22A10, SLC23A1, SLC25A1, SLC25A4, SLC28A1/CNT1, SLC29A4, SLC39A8, SLC35F4, SLC46A3	

Table 2. PFCA-mediated regulation of transporters in rodent livers
(b**old**: similar trend of regulation between the rodent data and the HepaRG human orthologs)

PFCAs	Species	Exposure time & dose	Transporters	Effect
PFOA	Mice	i.p. 80 mg/kg (livers were collected 48 h after exposure)	Abcc3/Mrp3, Abcc4/Mrp4	↑ (Maher et al., 2008)
		i.p. 40 mg/kg (livers were collected 48 h after exposure)	Slco1a1/Oatp1a1, Slco1a4/Oatp1a4, Slco1b2/Oatp1b2	↓ (Cheng and Klaassen, 2008a)
PFNA	Mice	i.p. 46.41 mg/kg (0.1 mmol/kg) single dose (livers were collected after 1 week)	Slc10a1/Ntcp, PPARα-dependent: Slco1a1/Oatp1a1, Slco1a4/Oatp1a4, Slco2b1/Oatp2b1, Slc22a7/Oat2, Abcb11/Bsep; CAR- and PPARα-dependent: Slco1b2/Oatp1b2	↓ (Zhang et al., 2018)
			Abcc3/Mrp3, Abcc4/Mrp4 PPARα-dependent: Abca1,Abcb4/Mdr2, Abcc2/Mrp2, Abcg1, **Abcg2/Bcrp**, Abcg5, Abcg8	↑ (Zhang et al., 2018)
PFDA	Rats	i.p. 40 mg/kg single dose (livers were collected 4 days later)	ABCC2/MRP2	↓ (Not statistically significant) (Johnson and Klaassen, 2002a)

	Mice	i.p. up to 80 mg/kg (wild type) 40 mg/kg (PPARα-null), livers were collected 48 h after exposure)	PPARα- and Nrf2-dependent & promoted by Kupffer cells: **Abcc3/Mrp3** (10, 20, 40, 80 mg/kg), Abcc4/Mrp4 (20, 40, 80 mg/kg)	↑ (Maher et al., 2008)
			Slco1a1/Oatp1a1 (40 & 80 mg/kg); PPARα-dependent (40 mg/kg): Slco1b2/Oatp1b2 (40 & 80 mg/kg), **Slc10a1/Ntcp** (10, 20, 40, 80 mg/kg); PPARα- (40 mg/kg) and PXR-dependent (80 mg/kg): Slco1a4/Oatp1a4 (0.5, 1, 10, 20, 40, 80 mg/kg)	↓ (Cheng and Klaassen, 2008a)

DISCUSSION

A previous study showed that PFOA down-regulated most detected transporters (Table 1) (Behr et al., 2020). The only up-regulated transporters reported were the cholesterol efflux transporter ABCG1 and the BA efflux transporter SLC51B/OSTβ (Table 1) (Behr et al., 2020). Most of the observations from the previous study (Behr et al., 2020) took place at higher PFOA concentrations and/or over a longer incubation time than the present study, with only a few exceptions (PFOA at 10 μM down-regulated ABCG5/G8, MRP3 and up-regulated OSTβ). Correspondingly, at these higher concentrations, PFOA in HepaRG cells increased the major hepatic BAs T-CA and G-CA (250 μM), dilated the bile canaliculi (100 μM), and down-regulated the CYP7A1 protein of the rate-limiting enzyme for BA synthesis (100 – 250 μM),

suggesting that PFOA has a cholestatic potential at sub-toxic concentrations (Behr et al., 2020). Therefore, although PFOA at the higher concentrations did not reduce HepaRG cell viability (Behr et al., 2020), it may increase cellular stress by disrupting lipid homeostasis. Thus the discrepancy between this previous study and the present study may be due to dose. Interestingly, in male rats, PFOA increased hepatic triglyceride levels and peroxisomal beta-oxidation between 10 and 20 mg/kg dose ranges (i.p. once daily for 5 days), corresponding to male-specific hepatic accumulation of PFOA (Kudo and Kawashima, 2003). Although the expression of transporters was not determined in the study done in rats (Kudo and Kawashima, 2003), it is possible that the down-regulation of efflux transporters involved in lipid homeostasis may contribute to increased hepatic triglyceride levels. Interestingly, PFOA-exposed mice (40 mg/kg, i.p.) also had decreased expression of several hepatic uptake transporters in the Slco family (Table 2) (Cheng and Klaassen, 2008a), among which Slco1b2/Oatp1b2 has been suggested to contribute to the hepatic uptake of unconjugated BAs (Csanaky et al., 2011). PFOA-exposed mice (40 mg/kg, i.p.) also had increased expression of hepatic efflux transporters Abcc3/Mrp3 and Abcc4/Mrp4 (Maher et al., 2008). These Mrp transporters transport drugs and can also transport BAs during cholestasis (Mennone et al., 2006). Both the down-regulation of uptake transporters and the up-regulation of efflux transporters suggest compensatory mechanisms to protect the hepatocytes from further toxic insults from PFOA exposure, and indicate that these doses used in mice may be at the higher end.

Although the lipid and drug transporters were not regulated by PFOA at the lower concentration of 45 μM in HepaRG cells from our study as compared to the literature (Behr et al., 2020), we observed consistent PFOA-mediated up-regulatory patterns for the genes for

amino acid transporters SLC1A4, SLC7A11, and the endoplasmic reticulum (ER) inorganic phosphate/glucose-6-phosphate antiporter SLC37A2 (Pan et al., 2011; Lin et al., 2015) at 24 h at both low (45 μM) and low (100 μM) concentrations (Louisse et al., 2020) (Table 1, Fig. 7-8). Thus, PFOA is important in promoting the expression of transporters involved in protein synthesis and ER functions. Several other SLC transporters were not consistently regulated between the present study and the literature (Table 1), and this is likely due to differences in PFOA concentrations, incubation times, and/or culture media components (Behr et al., 2020; Louisse et al., 2020).

A previous study showed that PFNA at a higher concentration (100 μM, 24h) up-regulated several amino acid transporters (SLC1A4, SLC1A5, SLC7A1, SLC7A5, and SLC7A11, and SLC43A1), the monocarboxylic acid transporter (SLC16A13, which transports lactate, pyruvate, branched-chain oxo acids derived from leucine, valine and isoleucine, as well as ketone bodies acetoacetate, beta-hydroxybutyrate and acetate), and the ER inorganic phosphate/glucose-6-phosphate antiporter SLC37A2 (Louisse et al., 2020). Interestingly, the present study showed that PFNA at the lower concentration of 45 μM (24 h) also up-regulated these transporters (Table 1). It is important to note that the amino acid transporters SLC1A4, SLC7A11, and SLC37A2 were consistently up-regulated by both PFOA and PFNA at both low and high concentrations (Louisse et al., 2020)(Table 1, Fig. 7). The consistency between the present study and the literature further confirmed the up-regulatory effect of PFNA and PFOA at multiple non-toxic concentrations on transporters that are important for protein synthesis.

To the best of our knowledge there are no reports on the effect of PFDA on the hepatic transcriptomic response in HepaRG cells. The present study has provided the first evidence

showing that, PFDA regulated the most numbers of genes in HepaRG cells than the other PFCA congeners, and most of these genes were uniquely regulated by PFDA but not the other 2 PFCA congeners (Fig. 1G and 1H). At the transcriptome-wide level, PFDA was also predicted to activate the most genes that are upstream regulators including transcription factors involved in in xenobiotic metabolism (NFE2L2/NRF2, NR1I3/CAR, NR1I2/PXR) and lipid metabolism (PPARA, PPARG, PPARD, PPARGC1A/PGC1α, NR1H4/FXR, and HNF4A), epigenetic modulators (HDAC1, HDAC2, EZH2), and steroid hormone nuclear receptors (PGR and ESR1), and the tumor suppressor TRP53/P53 (Fig. 4B). At the transporter level, PFDA regulated more genes for xenobiotic and BA transporters than the other PFCAs, and the up-regulation of xenobiotic efflux transporters and down-regulation of uptake transporters may suggest a protective mechanism to reduce further toxic insults. Indeed, it has been shown that PFDA exposure increased serum BA concentrations in mice (Cheng and Klaassen, 2008) ; whereas the PFOA-mediated down-regulation of the major BA hepatic uptake transporter SLCO10A1/NTCP in both HepaRG cells (Fig. 5B and Fig. 9) and mouse liver (Cheng and Klaassen, 2008) indicate a compensatory mechanism to prevent excessive BA accumulation in liver. In summary, among the 3 PFCA congeners tested, PFDA is the most potent on modulating the hepatic transcriptomic response in general and transporter gene expression in particular.

Similar to the inducible effect of amino acid transporters by PFOA and PFNA, PFDA exposure also up-regulated many genes associated with amino acid transporters, including SLC1A4, SLC1A5, SLC6A9, SLC7A1, SLC7A2, SLC7A5, SLC7A11, and SLC43A1, as well as the ER inorganic phosphate/glucose-6-phosphate antiporter SLC37A2 (Table 1) (Fig. 7). The present study is among the first to demonstrate that genes associated with amino acid

transporters, which are essential for protein synthesis, are a class of novel inducible targets by all 3 PFCAs (Table 1) (Louisse et al., 2020). This finding is further supported by the transcriptome-wide pathway analysis showing that all 3 PFCAs commonly up-regulated amino acid-related pathways including L-amino acid transport, tRNA for protein synthesis, amino acid activation, cellular amino acid metabolic process processes, and response to ER stress (Fig. 2-4). It has been increasingly recognized that understanding the role of amino acid intake in the pathogenesis of liver disease is a promising therapeutic strategy, because amino acids are involved in a wide spectrum of cellular metabolisms, including the synthesis of lipids and nucleotides as well as the chemical detoxification process (Lee and Kim, 2019). For example, amino acids have been suggested to protect against acetaminophen-induced hepatotoxicity by serving as mitochondrial energy substrates independent from glutathione synthesis in mice (Saito et al., 2010). Branched chain amino acids have been shown to suppress hepatocellular carcinoma *in vitro* and are required for immunosurveillance. In addition, in cirrhotic patients, serum branched chain amino acids (BCAA) are decreased, and administration of BCAA-rich medicine has shown positive results (Tajiri and Shimizu, 2018). PFNA and PFOA have been shown to produce hepatomegaly and peroxisomal b-oxidation (Kudo et al., 2006), and PFNA has been shown to increase hepatic triglyceride and total cholesterol as well as serum transaminase in mice (Wang et al., 2015). Very little is known regarding how transporter-mediated amino acid intake modifies PFCA-mediated hepatotoxicity. It is important to further investigate this in future studies.

A limitation of the present study is not assessing the PFCA concentrations in media. However, it is important to note that all three PFCAs are well-characterized substrates of the major hepatic uptake transporters NTCP (Ruggiero et al., 2021), which is a hepatocyte-specific

transporter. In addition, the liver-enriched transporters OATP1B1, 1B3, and 2B1 also contribute to the hepatic uptake of PFCAs (Zhao et al., 2017). Therefore, at the equal molar concentration of 45 μM, which is a relatively low concentration, the majority of the PFCA compounds are expected to be taken up into the hepatocytes rather than lingering in the media. A limitation of the present study is not assessing the PFCA concentrations in media. However, it is important to note that all three PFCAs are well-characterized substrates of the major hepatic uptake transporters NTCP (Ruggiero et al., 2021), which is a hepatocyte-specific transporter. In addition, the liver-enriched transporters OATP1B1, 1B3, and 2B1 also contribute to the hepatic uptake of PFCAs (Zhao et al., 2017). Therefore, at the equal molar concentration of 45 μM, which is a relatively low concentration, the majority of the PFCA compounds are expected to be taken up into the hepatocytes rather than lingering in the media. Another limitation of the present study was the focus on transcriptomic regulation without validation at the levels of protein expression and functional consequences. Because changes at the RNA level may not necessarily always translate into functional changes, additional studies in the figure are needed to address this limitation. Within the context of transporters, future studies are needed to quantify PFCA-mediated changes in both the protein abundance and the cellular localizations; in addition, intracellular and extracellular intermediary metabolites (such as amino acids) should be determined by metabolomics approach using in vitro and in vivo models. It is important to note that smaller changes in gene expression may or may not lead to physiological consequences. Therefore, cautions are needed while interpreting RNA-Seq data from limited sample size for functional output. In addition, RT-qPCR may be inherently biased because it is based on short primer sequences. For example, the discrepancy in OATP2B1 mRNA levels from RT-qPCR and

RNA-Seq results may be due to amplifying only portions of the mRNA regions (RT-qPCR) vs. estimating the mRNA abundance using reads from all exons (RNA-Seq).

Despite the difference in the potency of the 3 PFCAs in modulating the hepatic transcriptome, all 3 PFCAs were predicted to activate the genes associate with lipid-sensing nuclear receptor PPARα and the xenobiotic-sensing nuclear receptor NR1I2/PXR in HepaRG cells (Fig. 2-4). Consistent with this prediction in HepaRG cells, *in vivo* studies using nuclear receptor gene null mice showed that PPARα is necessary in the PFNA-mediated regulation of multiple xenobiotic transporters (Zhang et al., 2018), and both PPARα and PXR are necessary in the PFDA-mediated regulation of multiple transporters in liver (Cheng and Klaassen, 2008a) (Table 2). In addition to PPAR and NRF1I2/PXR, all 3 PFCAs were also predicted to activate the master regulator for lipid and drug metabolism – HNF4α, the hypoxia-inducible factor-1α (HIF1A) which is involved in liver fibrosis, inflammation and cancer (Nath and Szabo, 2012), as well as the activating transcription factor 4 (ATF4), which directs stress-induced gene expression in the unfolded protein response and cholesterol metabolism in the liver (Fusakio et al., 2016) (Fig. 2-4). Together these regulatory signatures may serve as early biomarkers for liver injury even at low doses of PFCA exposures.

CONCLUSION

The present study using PFOA ([C8]), PFNA ([C9]), and PFDA ([C10]) at a concentration lower than what was used in HepaRG cells from the literature showed that genes associated with amino acid transporters, which are critical for protein synthesis, are novel inducible targets for all 3 PFCAs. PFCAs with increasing carbon chain lengths had greater transcriptomic response in HepaRG cells, and the top commonly activated pathways are involved in amino acid metabolism and transport. Commonly activated or predicted to be activated genes for receptors include PPARα, CAR, PXR, and ATF4 by all PFCAs at the global level. At the transporter level, none of the PFCA-mediated transporter gene regulations appeared to be through PPARα or CAR but appeared to be through Nrf2. At equal molar concentration showed that PFCA congeners with a longer carbon chain length are more potent in regulating the expression of transporters for xenobiotics and BAs, and these results suggest a compensatory response to reduce exposures to PFCAs of longer carbon chains by increasing their efflux and reduce their further uptake. In addition, the amino acid transporters were regulated by all PFCAs, and these transporters are critical for protein synthesis and may contribute to chemical detoxification.

Taken together, the goal of the present study was to investigate the effect of PFCAs with various carbon chain lengths at an equal molar concentration on transporters involved in intermediary metabolism and xenobiotic biotransformation in human hepatocytes. From a transcriptome-wide scale, we also identified common and unique pathways regulated by various PFCAs, as predicted by the upstream regulators in an unbiased approach. Because it has been

shown in mouse models that certain PFCAs activate CAR and PPARα (Cheng et al., 2008a and 2008b) , the effects of the prototypical ligands for CAR (CITCO) and PPARα were also investigated. To note, WY-14643 has been primarily used as an activator of PPARα (Hsu et al., 1995; Devchand et al., 1996; Staels et al., 1998); however, it also activates PPARγ (Lehmann et al., 1997) and PPARδ, although this finding is rare (Schmidt et al., 1992). While all 3 PFCAs were shown to activate PPARα as evidenced by the up-regulation of CYP4A11 (Fig. S1) and upstream regulator analysis (Fig. S4A-C), PPARγ and PPARδ were also predicted upstream regulators for PFOA and PFDA exposures (Fig. S4). Therefore, the other PPAR receptors in addition to PPARα may also contribute to the transcriptomic response of HepaRG cells at the global level. However, at the transporter level, neither PPARα nor CAR appeared to be involved in the regulation of transporters by any of the PFCAs at the concentration used in the present study, because neither WY or CITCO regulated the transporters that were differentially regulated by PFCAs (Fig. 5B and Fig. 6-10). This is different from previous reports using livers from PFCA-exposed mice showing that PPARα are CAR are necessary in PFCA-mediated regulation of certain uptake and efflux transporter transporters (Cheng and Klaassen, 2008; Maher et al., 2008) (Table 2). This difference may be due to a lower concentration used in the present study, differences in the nuclear receptors between humans and mice, and/or *in vitro* vs. *in vivo* settings. However, interestingly, among all 3 PFCAs, the major oxidative stress sensor Nrf2 was predicted to be a common upstream regulator for transporters (Fig. S6). A previous report also showed that Nrf2 is necessary in modulating the PFDA-mediated up-regulation of Mrp3 and Mrp4 in mouse liver. This indicates that oxidative stress may be an important toxicological endpoint in PFCA-exposed hepatocytes. Indeed, it has been reported that oxidative stress and inflammation may

contribute to PFOA-induced hepatotoxicity in mice (Yang et al., 2014). In addition, PNFA has been shown to produce immunotoxicity and have persistent effects on the immune system (Rockwell et al., 2013; Rockwell et al., 2017), whereas Nrf2 is known to have an important immunomodulatory effect (Freeborn and Rockwell, 2021). Our study suggests that PFCAs may also activate Nrf2 to regulate the expression of transporters in human hepatocytes as a compensatory response.

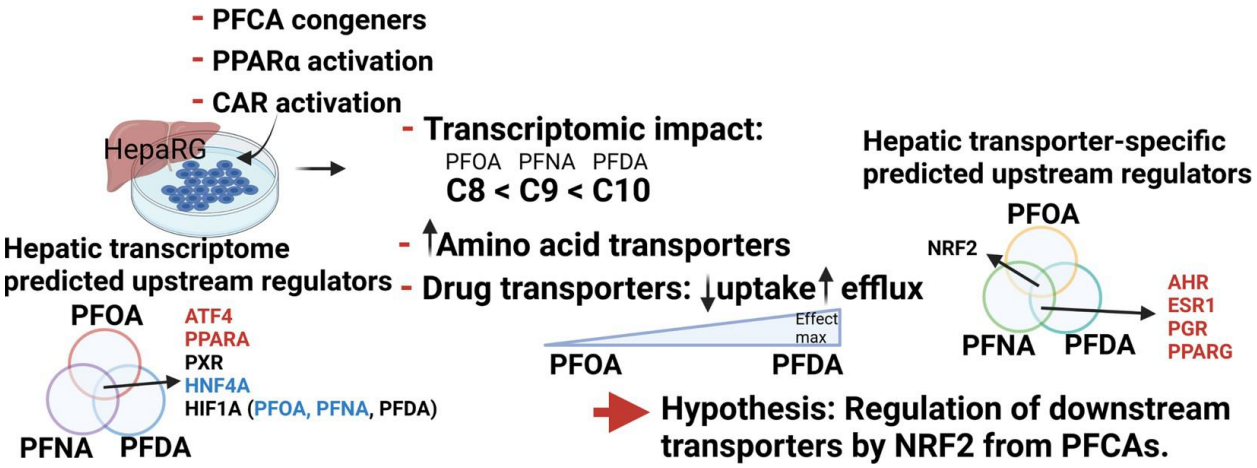

Figure 11. Diagram representing a summary of key findings and working hypothesis. In the present study, the transcriptomic changes from perfluorinated carboxylic acids (PFCAs) were investigated compared with CAR and peroxisome proliferator-activated receptor (PPAR)α activation. PFCAs altered the expression of genes involved in xenobiotic biotransformation (phase-I and -II metabolism, and transporters), as well as bile acid (BA), amino acid, and carbohydrate metabolism. The transcriptomic changes of PFCAs were correlated with the length of the carbon chains, with perfluorooctanoic acid having the least and perfluorodecanoic acid (PFDA) producing the greatest transcriptomic effect as evidenced by the number and degree of differentially regulated genes. Overall, at the transcriptome-wide scale, all PFCAs were predicted to activate AT F4 and P PARα and inhibit HNF4A. All P FCAs were also predicted to significantly modulate the P XR-signaling. perfluorooctanoic acid and PFNA were predicted to inhibit HIF1A (note: PFDA was also predicted to significantly modulate the HIF1A signaling). Regarding the transporters, NRF2 was predicted to be altered by all three PFCAs to regulate the transporter mRNAs. PFNA and PFDA were predicted to activate upstream regulators involved in xenobiotic biotransformation, signaling molecule regulation, and lipid sensing and metabolism (AHR, ESR1, P GR, and P PARG) to regulate the transporter mRNAs. Therefore, we hypothesize that key transcription factors, such as ATF4 and NRF2 play critical roles in regulating downstream signatures of xenobiotic, carbohydrates, and amino acid metabolism from PFCAs. Several categories of transporters were differentially regulated, including an upregulation in many amino acid transporters and several

xenobiotic efflux transporters, as well as a down-regulation of several xenobiotic and BA uptake transporters, with PFDA having the most potent effect.

SUPPLEMENTAL FIGUES AND LEGENDS

I. Supplemental figure legends

Fig. S1. RT-qPCR of CYP1A2, CYP2B6, CYP3A4, and CYP4A11 mRNAs in HepaRG cells exposed to vehicle (0.1% DMSO, n=3), WY (45 μM, n=2), CITCO (2 μM, n=2), PFOA (45 μM, n=3), PFNA ((45 μM, n=3), or PFDA ((45 μM, n=3) for 24 h. The primer sequences are shown in Table S1. Data are expressed as % of GAPDH, and asterisks indicate statistically significant differences as compared to the DMSO-exposed group (one-way ANOVA followed by Duncan's post hoc test, $p < 0.05$).

Fig. S2. A. PCA of the normalized and filtered gene expression matrix comparing all chemical groups used in the study. B. STRING network analysis of commonly differentially regulated genes comparing PFOA, PFNA, and PFDA. C. STRING network analysis and KEGG enrichment (BH-FDR < 0.05) of commonly differentially regulated genes comparing PFNA and PFDA. Differentially regulated genes (BH-FDR < 0.05 and absolute fold change > 1.5) were used.

Fig. S3. A. Volcano plot showing differentially regulated genes by CITCO compared to DMSO. B. Up-regulated gene ontology enrichment by CITCO. C. Volcano plot showing differentially regulated genes by WY compared to DMSO. D. Up-regulated gene ontology enrichment by WY. No significantly down-regulated gene ontology terms were observed for CITCO or WY. Differentially regulated genes (BH-FDR < 0.05 and absolute fold change > 1.5) were used.

Fig. S4. Predicted upstream regulators by PFOA (A), PFNA (B), and PFDA (C) (BH-FDR < 0.1). Red and blue indicate predicted activation and inhibition, respectively. Grey represents significance without activation status. Number of differentially regulated genes involved in phase -I (D), phase-II (E), transporters (F), bile acid metabolism (G), amino acid metabolism (H), and

carbohydrate metabolism (I). Differentially expressed genes (BH-FDR < 0.05 and absolute fold change > 1.5) were used.

Fig. S5. One-way hierarchical clustering of genes involved in bile acid and amino acid metabolism (A) and carbohydrate metabolism (B) by DMSO (Control), CITCO, WY, PFOA, PFNA, and PFDA. All differentially expressed genes at least by one exposure group were used for hierarchical clustering. Colored bars in heatmaps represent genes that are differentially regulated in a particular exposure group, i.e., CITCO – red, WY – blue, PFOA – yellow, PFNA – green, PFDA – purple.

Fig. S6. Predicted upstream regulators from differentially regulated transporters (BH-FDR < 0.1) by PFOA (A), PFNA (B), and PFDA (C). Red and blue indicate predicted activation and inhibition, respectively. Grey represents significance without activation status.

Fig. S7. Pie plot comparing the relative mRNA abundance of ABC transporters from various sub-families under basal conditions in HepaRG cells. The cumulative TPM values of all ABC transporters in a certain sub-family were added in each sample and the average value was obtained from the 3 technical replicates per sub-family. The Pie chart is visualized using Sigma Plot and the composition of each transporter sub-family is expressed as % of total mRNA abundance of all ABC transporters listed in Table S1.

Fig. S8. Pie plot comparing the relative mRNA abundance of other transport ATPases under basal conditions in HepaRG cells. The cumulative TPM values of all other transport ATPases transporters (excluding ABC transporters) in a certain sub-family were added in each sample and the average value was obtained from the 3 technical replicates per sub-family. The Pie chart is visualized using Sigma Plot and the composition of each transporter sub-family is expressed as % of total mRNA abundance of all transport ATPases (excluding ABC transporters) listed in Table S1.

Fig. S9. Pie plot comparing the relative mRNA abundance of the SLCO/OATP transporters under basal conditions in HepaRG cells. The cumulative TPM values of all SLCO/OATP

transporters in a certain sub-family were added in each sample and the average value was obtained from the 3 technical replicates per sub-family. The Pie chart is visualized using Sigma Plot and the composition of each transporter sub-family is expressed as % of total mRNA abundance of all SLCO/OATP transporters listed in Table S1.

Fig. S10. Pie plot comparing the relative mRNA abundance of other SLC transporters under basal conditions in HepaRG cells. The cumulative TPM values of all SLCO/OATP transporters in a certain sub-family were added in each sample and the average value was obtained from the 3 technical replicates per sub-family. The Pie chart is visualized using Sigma Plot and the composition of each transporter sub-family is expressed as % of total mRNA abundance of all SLCO/OATP transporters listed in Table S1.

Fig. S11. RT-qPCR of OATP2B1, MRP3, NTCP, NRF2, HNF4α, PXR, PPARα, and CAR mRNAs in HepaRG cells exposed to vehicle (0.1% DMSO, n=3), WY (45 μM, n=2), CITCO (2 μM, n=2), PFOA (45 μM, n=3), PFNA ((45 μM, n=3), or PFDA ((45 μM, n=3) for 24 h. The primer sequences are shown in Table S1. Data are expressed as % of GAPDH. a and b represent statistically significant post hoc groups (one-way ANOVA followed by Duncan's post hoc test, $p < 0.05$).

Fig. S1

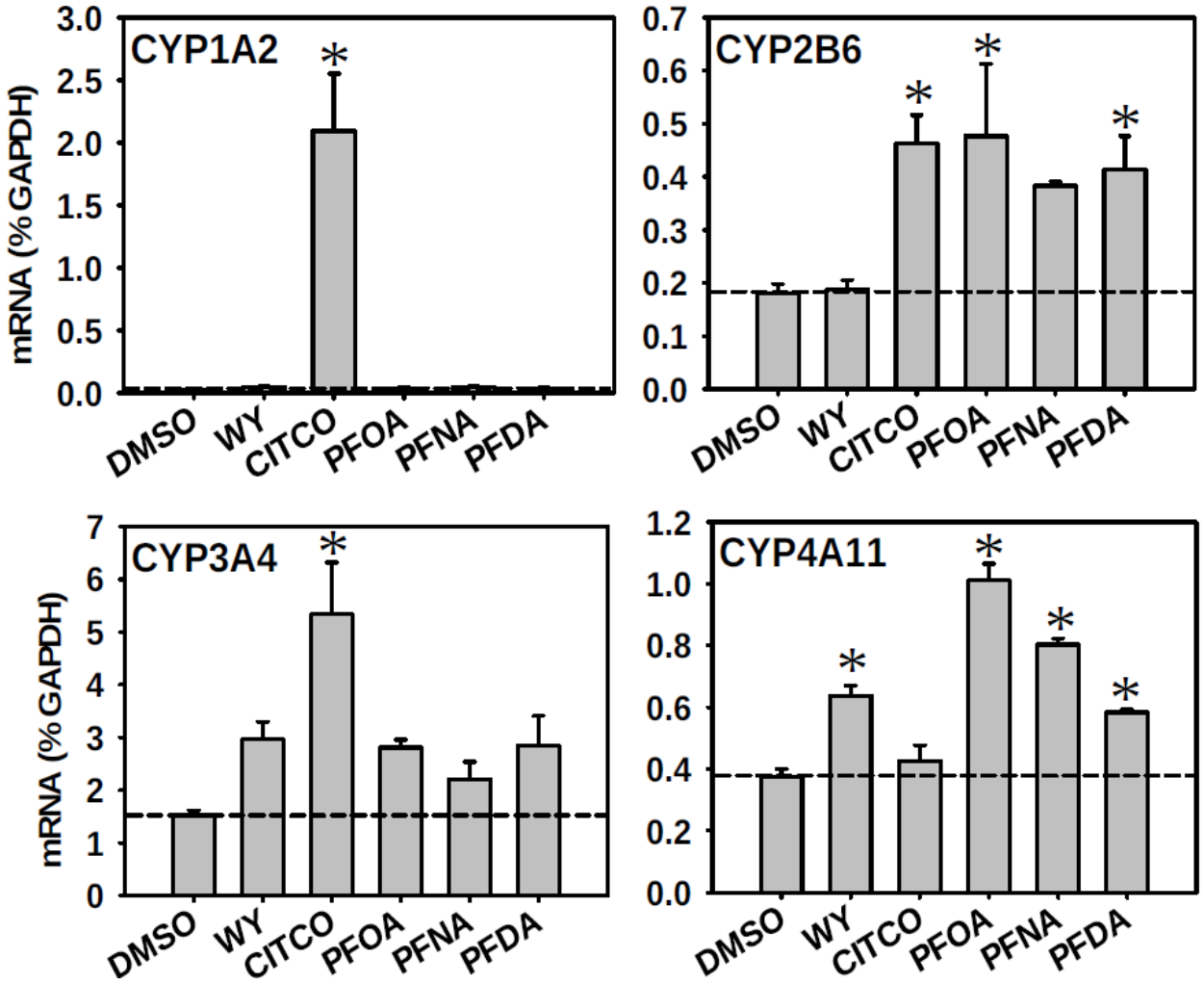
CYP1A2
CYP2B6
CYP3A4
CYP4A11
mRNA (% GAPDH)
DMSO
WY
CITCO
PFOA
PFNA
PFDA

Fig. S2

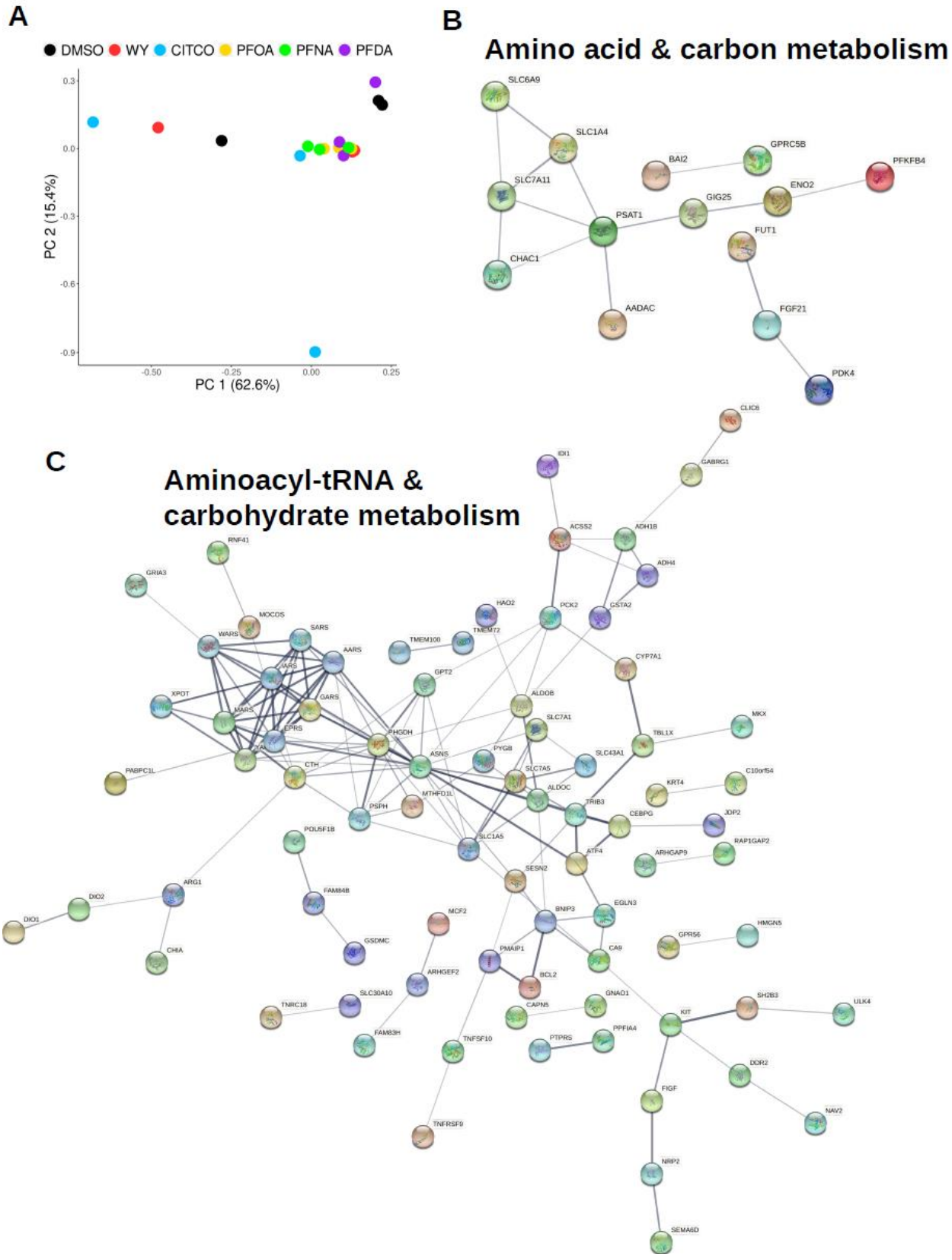
A
DMSO WY CITCO PFOA PFNA PFDA
PC 2 (15.4%)
PC 1 (62.6%)
B
Amino acid & carbon metabolism
SLC6A9
SLC1A4
BAI2
GPRC5B
PFKFB4
SLC7A11
ENO2
GIG25
PSAT1
FUT1
CHAC1
AADAC
FGF21
PDK4
C
Aminoacyl-tRNA &
carbohydrate metabolism
CLIC6
GABRG1
ACSS2
ADH1B
ADH4
RNF41
GRIA3
MOCOS
HAO2
PCK2
GSTA2
SARS
WARS
TMEM100
TMEM72
AARS
CYP7A1
GPT2
XPOT
ALDOB
GARS
SLC7A1
MKX
EPRS
PHGDH
TBL1X
PYGB
SLC43A1
PABPC1L
CTH
ASNS
SLC7A5
C10orf54
KRT4
ALDOC
MTHFD1L
TRIB3
PSPH
CEBPG
JDP2
POU5F1B
SLC1A5
RAP1GAP2
ATF4
ARHGAP9
SESN2
ARG1
DIO2
FAM84B
EGLN3
BNIP3
DIO1
MCF2
HMGN5
GPR56
GSDMC
PMAIP1
CA9
CHIA
ARHGEF2
BCL2
SLC30A10
GNAO1
SH2B3
ULK4
TNRC18
CAPN5
KIT
FAM83H
PPFIA4
TNFSF10
PTPRS
DDR2
FIGF
NAV2
TNFRSF9
NRP2
SEMA6D

Fig. S3

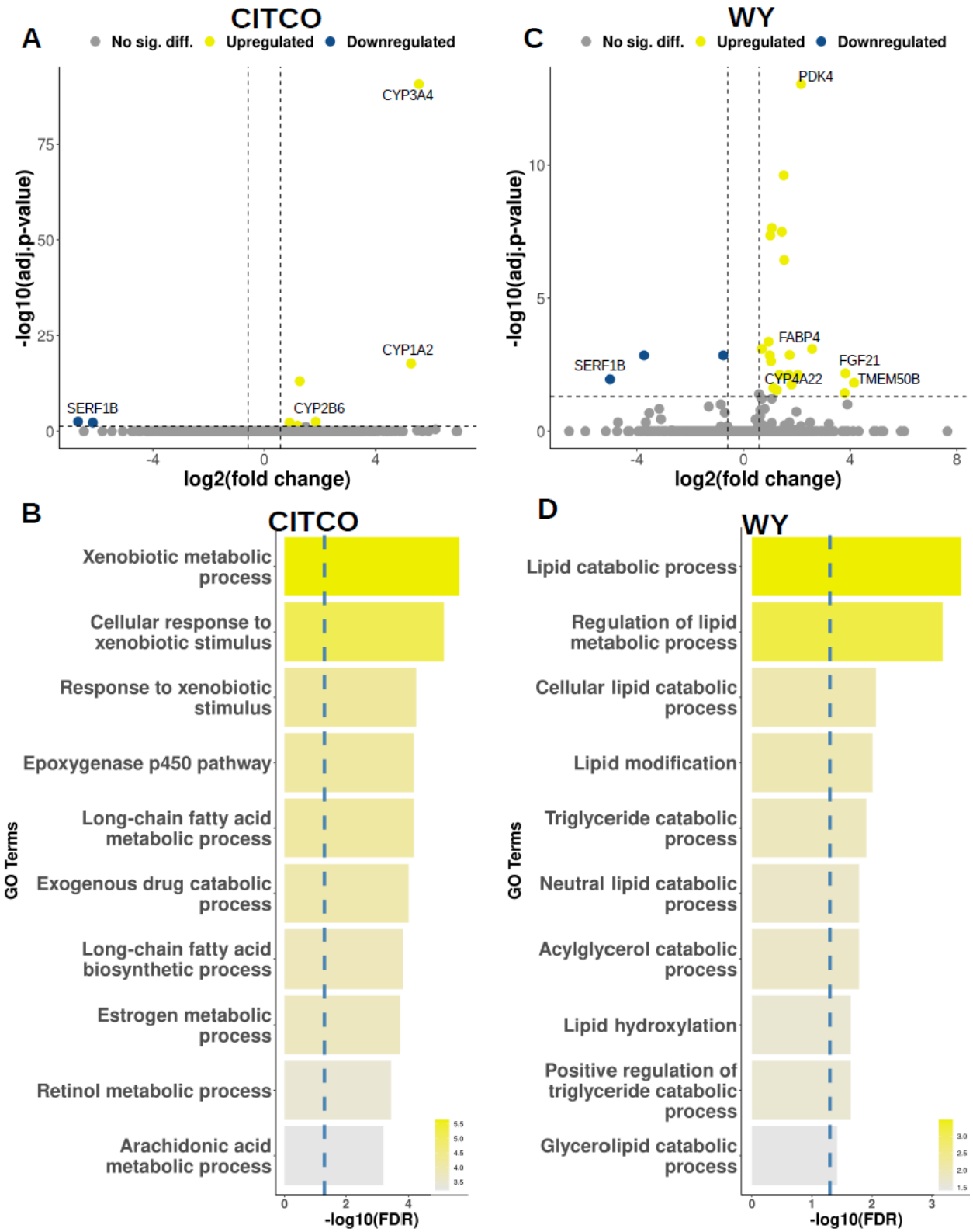
A
CITCO
No sig. diff.
Upregulated
Downregulated
CYP3A4
CYP1A2
CYP2B6
SERF1B
-log10(adj.p-value)
log2(fold change)
C
WY
PDK4
FABP4
FGF21
CYP4A22
TMEM50B
SERF1B
B
CITCO
Xenobiotic metabolic process
Cellular response to xenobiotic stimulus
Response to xenobiotic stimulus
Epoxygenase p450 pathway
Long-chain fatty acid metabolic process
Exogenous drug catabolic process
Long-chain fatty acid biosynthetic process
Estrogen metabolic process
Retinol metabolic process
Arachidonic acid metabolic process
GO Terms
-log10(FDR)
D
WY
Lipid catabolic process
Regulation of lipid metabolic process
Cellular lipid catabolic process
Lipid modification
Triglyceride catabolic process
Neutral lipid catabolic process
Acylglycerol catabolic process
Lipid hydroxylation
Positive regulation of triglyceride catabolic process
Glycerolipid catabolic process
GO Terms
-log10(FDR)

Fig. S4

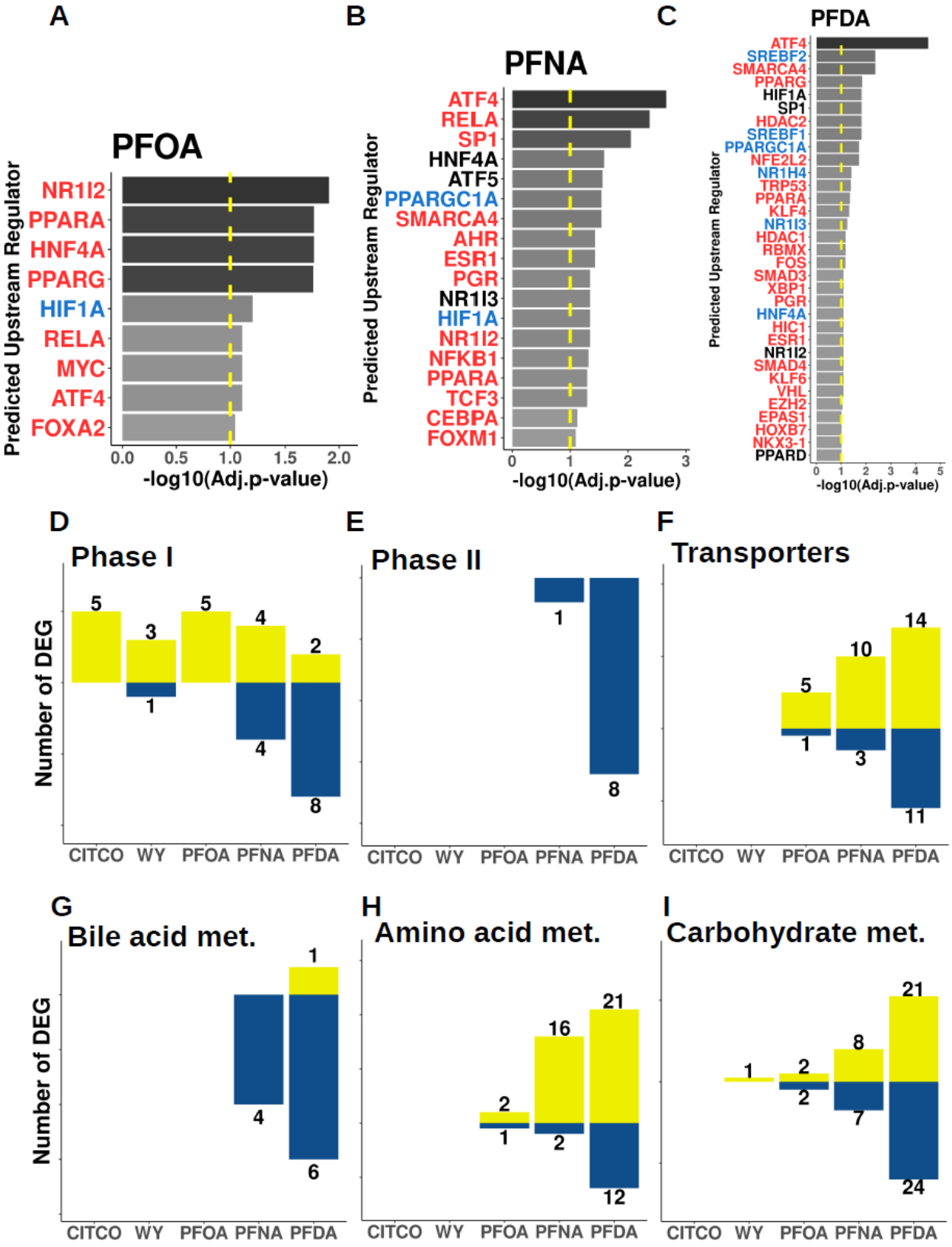
A
PFOA
Predicted Upstream Regulator
NR1I2
PPARA
HNF4A
PPARG
HIF1A
RELA
MYC
ATF4
FOXA2
0.0 0.5 1.0 1.5 2.0
-log10(Adj.p-value)
B
PFNA
Predicted Upstream Regulator
ATF4
RELA
SP1
HNF4A
ATF5
PPARGC1A
SMARCA4
AHR
ESR1
PGR
NR1I3
HIF1A
NR1I2
NFKB1
PPARA
TCF3
CEBPA
FOXM1
0 1 2 3
-log10(Adj.p-value)
C
PFDA
Predicted Upstream Regulator
ATF4
SREBF2
SMARCA4
PPARG
HIF1A
SP1
HDAC2
SREBF1
PPARGC1A
NFE2L2
NR1H4
TRP53
PPARA
KLF4
NR1I3
HDAC1
RBMX
FOS
SMAD3
XBP1
PGR
HNF4A
HIC1
ESR1
NR1I2
SMAD4
KLF6
VHL
EZH2
EPAS1
HOXB7
NKX3-1
PPARD
0 1 2 3 4 5
-log10(Adj.p-value)
D
Phase I
Number of DEG
5 3 5 4 2
1 4 8
CITCO WY PFOA PFNA PFDA
E
Phase II
1 8
CITCO WY PFOA PFNA PFDA
F
Transporters
5 10 14
1 3 11
CITCO WY PFOA PFNA PFDA
G
Bile acid met.
Number of DEG
1
4 6
CITCO WY PFOA PFNA PFDA
H
Amino acid met.
2 16 21
1 2 12
CITCO WY PFOA PFNA PFDA
I
Carbohydrate met.
1 2 8 21
2 7 24
CITCO WY PFOA PFNA PFDA

Fig. S5

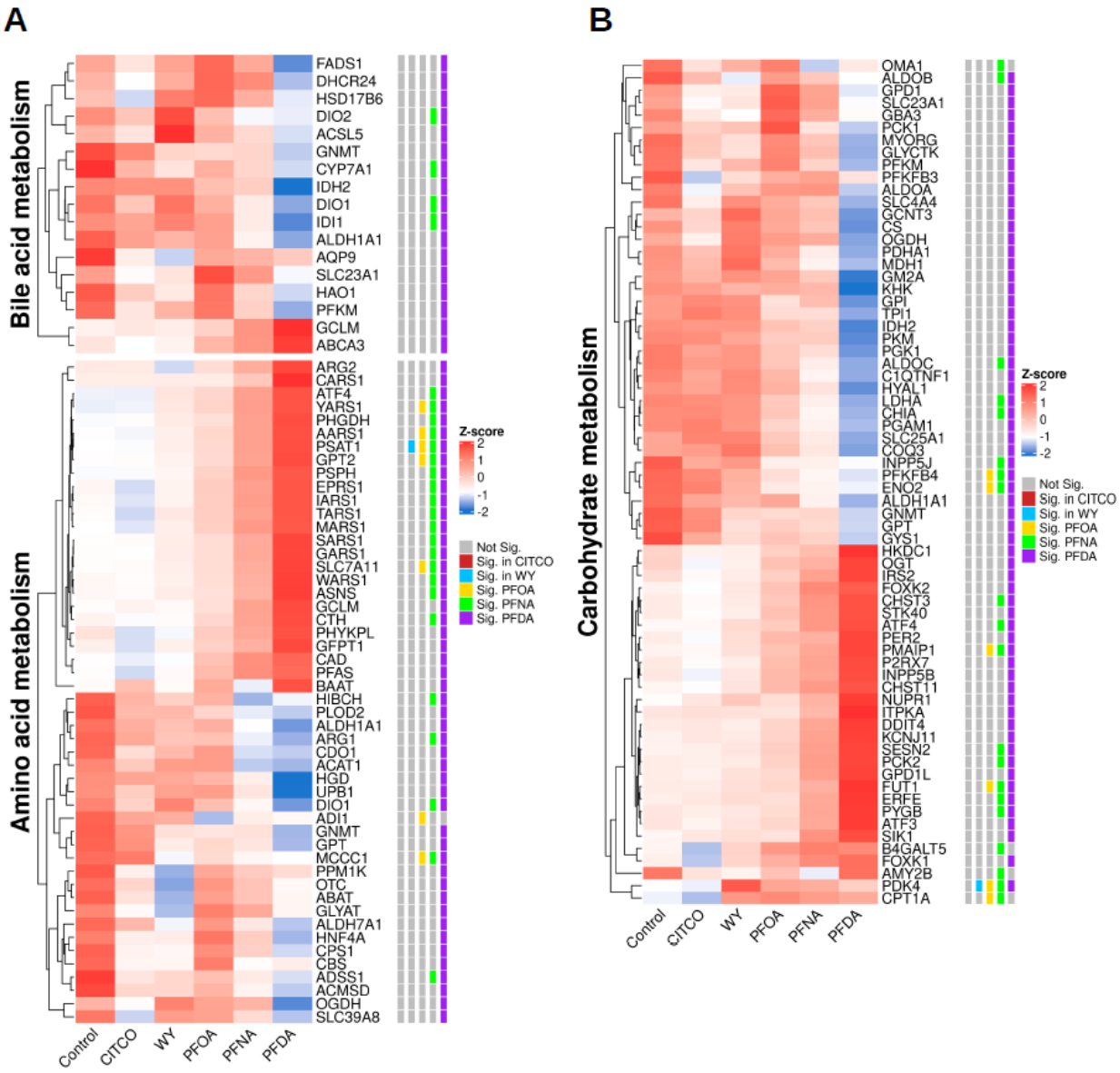
A
Bile acid metabolism
FADS1
DHCR24
HSD17B6
DIO2
ACSL5
GNMT
CYP7A1
IDH2
DIO1
IDI1
ALDH1A1
AQP9
SLC23A1
HAO1
PFKM
GCLM
ABCA3
Amino acid metabolism
ARG2
CARS1
ATF4
YARS1
PHGDH
AARS1
PSAT1
GPT2
PSPH
EPRS1
IARS1
TARS1
MARS1
SARS1
GARS1
SLC7A11
WARS1
ASNS
GCLM
CTH
PHYKPL
GFPT1
CAD
PFAS
BAAT
HIBCH
PLOD2
ALDH1A1
ARG1
CDO1
ACAT1
HGD
UPB1
DIO1
ADI1
GNMT
GPT
MCCC1
PPM1K
OTC
ABAT
GLYAT
ALDH7A1
HNF4A
CPS1
CBS
ADSS1
ACMSD
OGDH
SLC39A8
Control
CITCO
WY
PFOA
PFNA
PFDA
Z-score
2
1
0
-1
-2
Not Sig.
Sig. in CITCO
Sig. in WY
Sig. PFOA
Sig. PFNA
Sig. PFDA
B
Carbohydrate metabolism
OMA1
ALDOB
GPD1
SLC23A1
GBA3
PCK1
MYORG
GLYCTK
PFKM
PFKFB3
ALDOA
SLC4A4
GCNT3
CS
OGDH
PDHA1
MDH1
GM2A
KHK
GPI
TPI1
IDH2
PKM
PGK1
ALDOC
C1QTNF1
HYAL1
LDHA
CHIA
PGAM1
SLC25A1
COQ3
INPP5J
PFKFB4
ENO2
ALDH1A1
GNMT
GPT
GYS1
HKDC1
OGT
IRS2
FOXK2
CHST3
STK40
ATF4
PER2
PMAIP1
P2RX7
INPP5B
CHST11
NUPR1
ITPKA
DDIT4
KCNJ11
SESN2
PCK2
GPD1L
FUT1
ERFE
PYGB
ATF3
SIK1
B4GALT5
FOXK1
AMY2B
PDK4
CPT1A
Control
CITCO
WY
PFOA
PFNA
PFDA
Z-score
2
1
0
-1
-2
Not Sig.
Sig. in CITCO
Sig. in WY
Sig. PFOA
Sig. PFNA
Sig. PFDA

Fig. S6

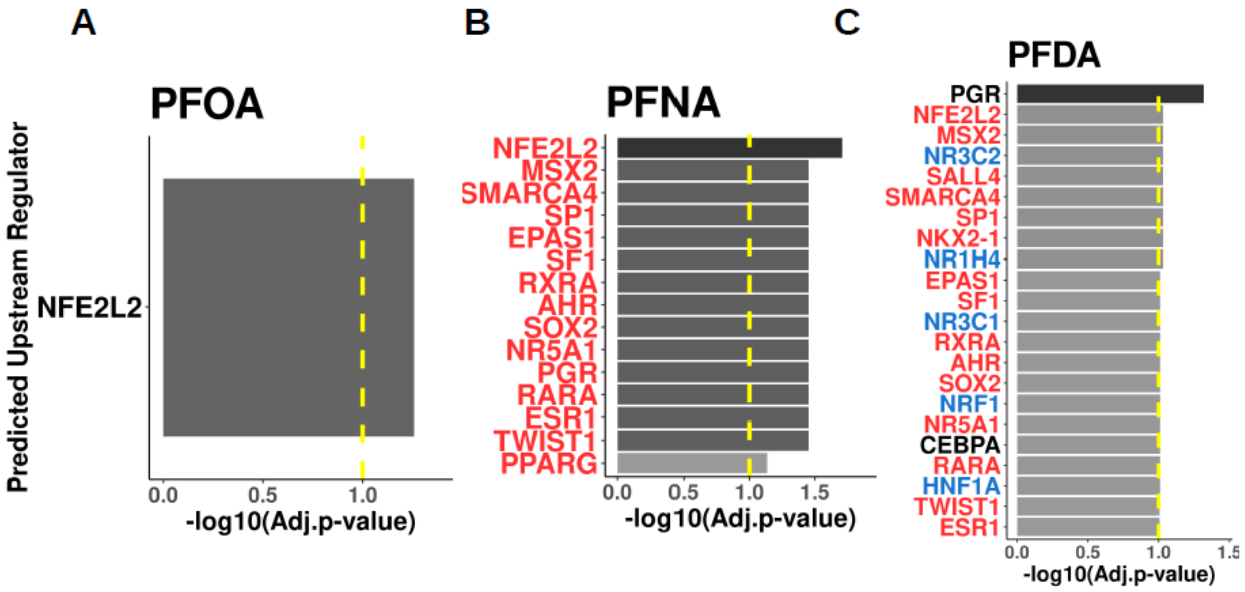
A
PFOA
Predicted Upstream Regulator
NFE2L2
0.0
0.5
1.0
-log10(Adj.p-value)
B
PFNA
NFE2L2
MSX2
SMARCA4
SP1
EPAS1
SF1
RXRA
AHR
SOX2
NR5A1
PGR
RARA
ESR1
TWIST1
PPARG
0.0
0.5
1.0
1.5
-log10(Adj.p-value)
C
PFDA
PGR
NFE2L2
MSX2
NR3C2
SALL4
SMARCA4
SP1
NKX2-1
NR1H4
EPAS1
SF1
NR3C1
RXRA
AHR
SOX2
NRF1
NR5A1
CEBPA
RARA
HNF1A
TWIST1
ESR1
0.0
0.5
1.0
-log10(Adj.p-value)

Fig. S7

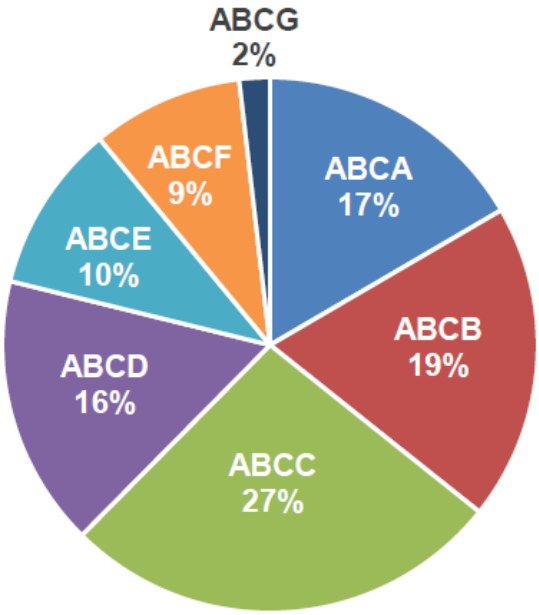
ABCG
2%
ABCA
17%
ABCB
19%
ABCC
27%
ABCD
16%
ABCE
10%
ABCF
9%

Fig. S8

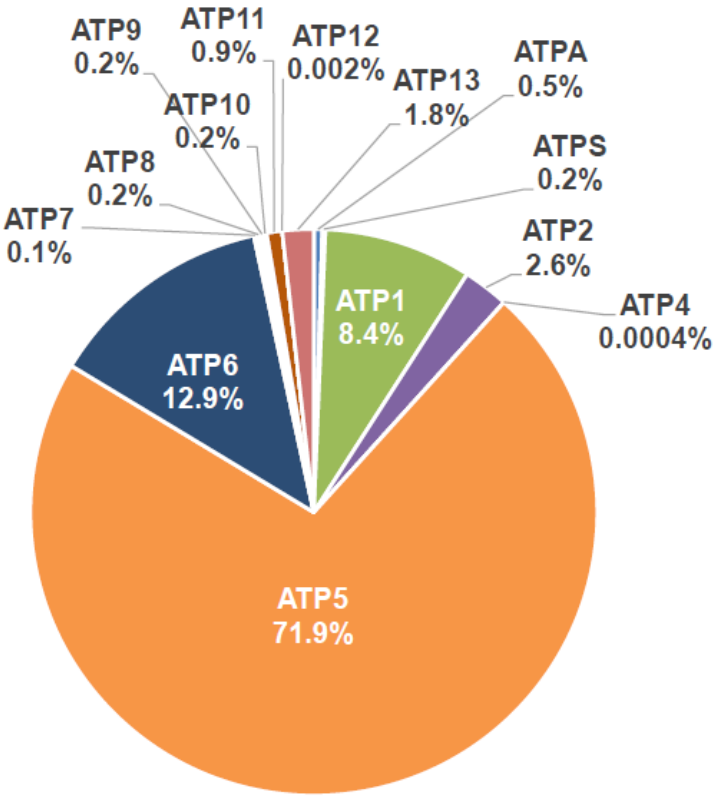
ATP9
0.2%
ATP11
0.9%
ATP12
0.002%
ATP13
1.8%
ATPA
0.5%
ATP10
0.2%
ATPS
0.2%
ATP8
0.2%
ATP7
0.1%
ATP2
2.6%
ATP4
0.0004%
ATP1
8.4%
ATP6
12.9%
ATP5
71.9%

Fig. S9

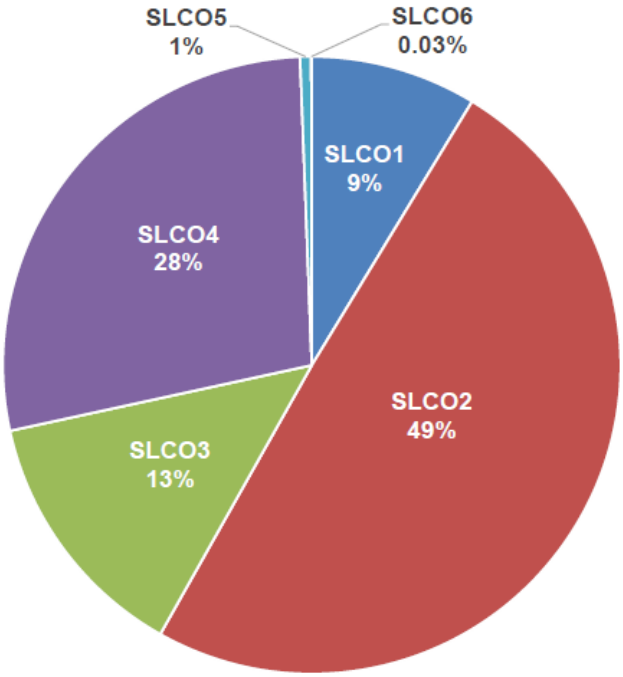

Fig. S10

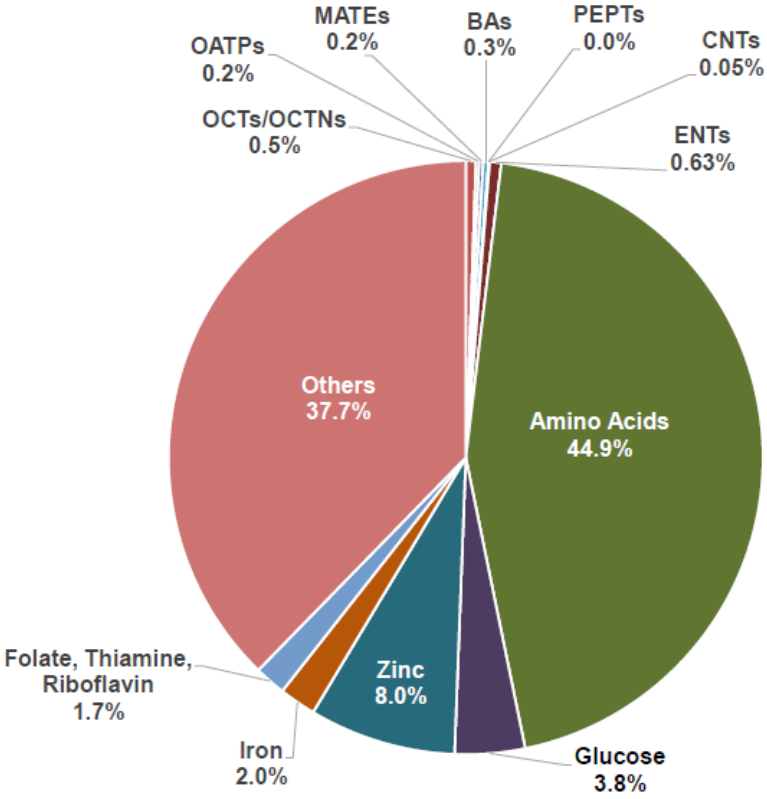

Fig. S11

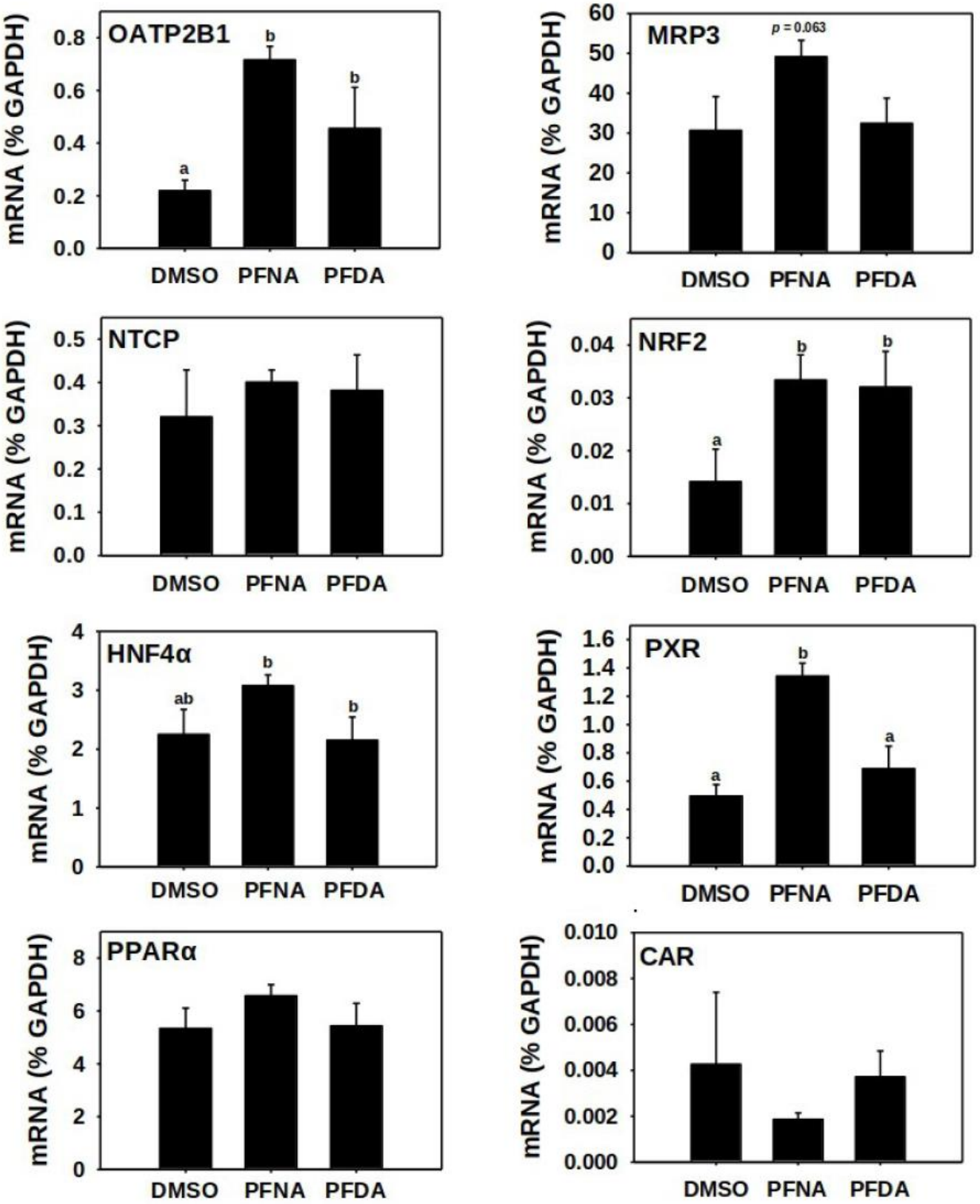
OATP2B1
mRNA (% GAPDH)
0.0
0.2
0.4
0.6
0.8
a
b
b
DMSO
PFNA
PFDA
MRP3
p = 0.063
mRNA (% GAPDH)
0
10
20
30
40
50
60
DMSO
PFNA
PFDA
NTCP
mRNA (% GAPDH)
0.0
0.1
0.2
0.3
0.4
0.5
DMSO
PFNA
PFDA
NRF2
mRNA (% GAPDH)
0.00
0.01
0.02
0.03
0.04
a
b
b
DMSO
PFNA
PFDA
HNF4α
mRNA (% GAPDH)
0
1
2
3
4
ab
b
b
DMSO
PFNA
PFDA
PXR
mRNA (% GAPDH)
0.0
0.2
0.4
0.6
0.8
1.0
1.2
1.4
1.6
a
b
a
DMSO
PFNA
PFDA
PPARα
mRNA (% GAPDH)
0
2
4
6
8
DMSO
PFNA
PFDA
CAR
mRNA (% GAPDH)
0.000
0.002
0.004
0.006
0.008
0.010
DMSO
PFNA
PFDA

REFERENCE

Alexa A, Rahnenfuhrer J (2021). *topGO: Enrichment Analysis for Gene Ontology*. R package version 2.44.0.

Wickham H (2016). *ggplot2: Elegant Graphics for Data Analysis*. Springer-Verlag New York. ISBN 978-3-319-24277-4, https://ggplot2.tidyverse.org.

Abe T, Takahashi M, Kano M, Amaike Y, Ishii C, Maeda K, Kudoh Y, Morishita T, Hosaka T, Sasaki T, Kodama S, Matsuzawa A, Kojima H, and Yoshinari K (2017) Activation of nuclear receptor CAR by an environmental pollutant perfluorooctanoic acid. *Arch Toxicol* **91:**2365-2374.

Adinehzadeh M and Reo NV (1998) Effects of peroxisome proliferators on rat liver phospholipids: sphingomyelin degradation may be involved in hepatotoxic mechanism of perfluorodecanoic acid. *Chem Res Toxicol* **11:**428-440.

Aleksunes LM and Klaassen CD (2012) Coordinated regulation of hepatic phase I and II drug-metabolizing genes and transporters using AhR-, CAR-, PXR-, PPARαlpha-, and Nrf2-null mice. *Drug Metab Dispos* **40:**1366-1379.

Almazroo OA, Miah MK, and Venkataramanan R (2017) Drug Metabolism in the Liver. *Clin Liver Dis* **21:**1-20.

Alnouti Y and Klaassen CD (2008a) Regulation of sulfotransferase enzymes by prototypical microsomal enzyme inducers in mice. *J Pharmacol Exp Ther* **324:**612-621.

Alnouti Y and Klaassen CD (2008b) Tissue distribution, ontogeny, and regulation of aldehyde dehydrogenase (Aldh) enzymes mRNA by prototypical microsomal enzyme inducers in mice. *Toxicol Sci* **101:**51-64.

Babu E, Kanai Y, Chairoungdua A, Kim DK, Iribe Y, Tangtrongsup S, Jutabha P, Li Y, Ahmed N, Sakamoto S, Anzai N, Nagamori S, and Endou H (2003) Identification of a novel system L amino acid transporter structurally distinct from heterodimeric amino acid transporters. *J Biol Chem* **278:**43838-43845.

Behr AC, Kwiatkowski A, Stahlman M, Schmidt FF, Luckert C, Braeuning A, and Buhrke T (2020) Impairment of bile acid metabolism by perfluorooctanoic acid (PFOA) and perfluorooctanesulfonic acid (PFOS) in human HepaRG hepatoma cells. *Arch Toxicol* **94:**1673-1686.

Boisvert G, Sonne C, Riget FF, Dietz R, and Letcher RJ (2019) Bioaccumulation and biomagnification of perfluoroalkyl acids and precursors in East Greenland polar bears and their ringed seal prey. *Environ Pollut* **252:**1335-1343.

Brady JM, Cherrington NJ, Hartley DP, Buist SC, Li N, and Klaassen CD (2002) Tissue distribution and chemical induction of multiple drug resistance genes in rats. *Drug Metab Dispos* **30:**838-844.

Buckley DB and Klaassen CD (2009) Induction of mouse UDP-glucuronosyltransferase mRNA expression in liver and intestine by activators of aryl-hydrocarbon receptor, constitutive androstane receptor, pregnane X receptor, peroxisome proliferator-activated receptor alpha, and nuclear factor erythroid 2-related factor 2. *Drug Metab Dispos* **37:**847-856.

Buhrke T, Kibellus A, and Lampen A (2013) In vitro toxicological characterization of perfluorinated carboxylic acids with different carbon chain lengths. *Toxicol Lett* **218:**97-104.

Calafat AM, Kuklenyik Z, Caudill SP, Reidy JA, and Needham LL (2006) Perfluorochemicals in pooled serum samples from United States residents in 2001 and 2002. *Environ Sci Technol* **40:**2128-2134.

Chen C and Klaassen CD (2004) Rat multidrug resistance protein 4 (Mrp4, Abcc4): molecular cloning, organ distribution, postnatal renal expression, and chemical inducibility. *Biochem Biophys Res Commun* **317:**46-53.

Chen C, Staudinger JL, and Klaassen CD (2003) Nuclear receptor, pregname X receptor, is required for induction of UDP-glucuronosyltranferases in mouse liver by pregnenolone-16 alpha-carbonitrile. *Drug Metab Dispos* **31:**908-915.

Chen EY, Tan CM, Kou Y, Duan Q, Wang Z, Meirelles GV, Clark NR, and Ma'ayan A (2013) Enrichr: interactive and collaborative HTML5 gene list enrichment analysis tool. *BMC Bioinformatics* **14:**128.

Chen H and Boutros PC (2011) VennDiagram: a package for the generation of highly-customizable Venn and Euler diagrams in R. *BMC Bioinformatics* **12:**35.

Cheng X, Buckley D, and Klaassen CD (2007) Regulation of hepatic bile acid transporters Ntcp and Bsep expression. *Biochem Pharmacol* **74:**1665-1676.

Cheng X and Klaassen CD (2008a) Critical role of PPAR-alpha in perfluorooctanoic acid- and perfluorodecanoic acid-induced downregulation of Oatp uptake transporters in mouse livers. *Toxicol Sci* **106:**37-45.

Cheng X and Klaassen CD (2008b) Perfluorocarboxylic acids induce cytochrome P450 enzymes in mouse liver through activation of PPAR-alpha and CAR transcription factors. *Toxicol Sci* **106:**29-36.

Cheng X, Maher J, Dieter MZ, and Klaassen CD (2005) Regulation of mouse organic anion-transporting polypeptides (Oatps) in liver by prototypical microsomal enzyme inducers that activate distinct transcription factor pathways. *Drug Metab Dispos* **33:**1276-1282.

Cherrington NJ, Hartley DP, Li N, Johnson DR, and Klaassen CD (2002) Organ distribution of multidrug resistance proteins 1, 2, and 3 (Mrp1, 2, and 3) mRNA and hepatic induction of Mrp3 by constitutive androstane receptor activators in rats. *J Pharmacol Exp Ther* **300:**97-104.

Cherrington NJ, Slitt AL, Maher JM, Zhang XX, Zhang J, Huang W, Wan YJ, Moore DD, and Klaassen CD (2003) Induction of multidrug resistance protein 3 (mrp3) in vivo is independent of constitutive androstane receptor. *Drug Metab Dispos* **31:**1315-1319.

Conney AH (1967) Pharmacological implications of microsomal enzyme induction. *Pharmacol Rev* **19:**317-366.

Csanaky IL, Lu H, Zhang Y, Ogura K, Choudhuri S, and Klaassen CD (2011) Organic anion-transporting polypeptide 1b2 (Oatp1b2) is important for the hepatic uptake of unconjugated bile acids: Studies in Oatp1b2-null mice. *Hepatology* **53:**272-281.

Cui JY and Klaassen CD (2016) RNA-Seq reveals common and unique PXR- and CAR-target gene signatures in the mouse liver transcriptome. *Biochim Biophys Acta* **1859:**1198-1217.

Cui YJ, Cheng X, Weaver YM, and Klaassen CD (2009) Tissue distribution, gender-divergent expression, ontogeny, and chemical induction of multidrug resistance transporter genes (Mdr1a, Mdr1b, Mdr2) in mice. *Drug Metab Dispos* **37:**203-210.

De Silva AO and Mabury SA (2006) Isomer distribution of perfluorocarboxylates in human blood: potential correlation to source. *Environ Sci Technol* **40:**2903-2909.

Devchand PR, Keller H, Peters JM, Vazquez M, Gonzalez FJ, and Wahli W (1996) The PPARαlpha-leukotriene B4 pathway to inflammation control. *Nature* **384:**39-43.

Dieter MZ, Maher JM, Cheng X, and Klaassen CD (2004) Expression and regulation of the sterol half-transporter genes ABCG5 and ABCG8 in rats. *Comp Biochem Physiol C Toxicol Pharmacol* **139:**209-218.

Doring B and Petzinger E (2014) Phase 0 and phase III transport in various organs: combined concept of phases in xenobiotic transport and metabolism. *Drug Metab Rev* **46:**261-282.

Eggers Pedersen K, Basu N, Letcher R, Greaves AK, Sonne C, Dietz R, and Styrishave B (2015) Brain region-specific perfluoroalkylated sulfonate (PFSA) and carboxylic acid (PFCA) accumulation and neurochemical biomarker responses in east Greenland polar bears (Ursus maritimus). *Environ Res* **138:**22-31.

Falandysz J, Taniyasu S, Gulkowska A, Yamashita N, and Schulte-Oehlmann U (2006) Is fish a major source of fluorinated surfactants and repellents in humans living on the Baltic Coast? *Environ Sci Technol* **40:**748-751.

Freeborn RA and Rockwell CE (2021) The role of Nrf2 in autoimmunity and infectious disease: Therapeutic possibilities. *Adv Pharmacol* **91:**61-110.

Fujii Y, Niisoe T, Harada KH, Uemoto S, Ogura Y, Takenaka K, and Koizumi A (2015) Toxicokinetics of perfluoroalkyl carboxylic acids with different carbon chain lengths in mice and humans. *J Occup Health* **57:**1-12.

Fusakio ME, Willy JA, Wang Y, Mirek ET, Al Baghdadi RJ, Adams CM, Anthony TG, and Wek RC (2016) Transcription factor ATF4 directs basal and stress-induced gene

expression in the unfolded protein response and cholesterol metabolism in the liver. *Mol Biol Cell* **27:**1536-1551.

Gerbal-Chaloin S, Briolotti P, Daujat-Chavanieu M, and Rasmussen MK (2021) Primary hepatocytes isolated from human and porcine donors display similar patterns of cytochrome p450 expression following exposure to prototypical activators of AhR, CAR and PXR. *Curr Res Toxicol* **2:**149-158.

Gottesman MM and Ling V (2006) The molecular basis of multidrug resistance in cancer: the early years of P-glycoprotein research. *FEBS Lett* **580:**998-1009.

Gregus Z, Madhu C, and Klaassen CD (1990) Effect of microsomal enzyme inducers on biliary and urinary excretion of acetaminophen metabolites in rats. Decreased hepatobiliary and increased hepatovascular transport of acetaminophen-glucuronide after microsomal enzyme induction. *Drug Metab Dispos* **18:**10-19.

Gu Z, Eils R, and Schlesner M (2016) Complex heatmaps reveal patterns and correlations in multidimensional genomic data. *Bioinformatics* **32:**2847-2849.

Guo GL, Choudhuri S, and Klaassen CD (2002) Induction profile of rat organic anion transporting polypeptide 2 (oatp2) by prototypical drug-metabolizing enzyme inducers that activate gene expression through ligand-activated transcription factor pathways. *J Pharmacol Exp Ther* **300:**206-212.

Guruge KS, Yeung LW, Yamanaka N, Miyazaki S, Lam PK, Giesy JP, Jones PD, and Yamashita N (2006) Gene expression profiles in rat liver treated with perfluorooctanoic acid (PFOA). *Toxicol Sci* **89:**93-107.

Hagenbuch B and Meier PJ (2004) Organic anion transporting polypeptides of the OATP/ SLC21 family: phylogenetic classification as OATP/ SLCO superfamily, new nomenclature and molecular/functional properties. *Pflugers Arch* **447:**653-665.

Han H, Cho JW, Lee S, Yun A, Kim H, Bae D, Yang S, Kim CY, Lee M, Kim E, Lee S, Kang B, Jeong D, Kim Y, Jeon HN, Jung H, Nam S, Chung M, Kim JH, and Lee I (2018) TRRUST v2: an expanded reference database of human and mouse transcriptional regulatory interactions. *Nucleic Acids Res* **46:**D380-D386.

Han X, Yang CH, Snajdr SI, Nabb DL, and Mingoia RT (2008) Uptake of perfluorooctanoate in freshly isolated hepatocytes from male and female rats. *Toxicol Lett* **181:**81-86.

Heindel JJ, Blumberg B, Cave M, Machtinger R, Mantovani A, Mendez MA, Nadal A, Palanza P, Panzica G, Sargis R, Vandenberg LN, and Vom Saal F (2017) Metabolism disrupting chemicals and metabolic disorders. *Reprod Toxicol* **68:**3-33.

Hood A and Klaassen CD (2000) Effects of microsomal enzyme inducers on outer-ring deiodinase activity toward thyroid hormones in various rat tissues. *Toxicol Appl Pharmacol* **163:**240-248.

Jarvis AL, Justice JR, Elias MC, Schnitker B, and Gallagher K (2021) Perfluorooctane Sulfonate in US Ambient Surface Waters: A Review of Occurrence in Aquatic Environments and Comparison to Global Concentrations. *Environ Toxicol Chem* **40:**2425-2442.

Hsu MH, Palmer CN, Griffin KJ, and Johnson EF (1995) A single amino acid change in the mouse peroxisome proliferator-activated receptor alpha alters transcriptional responses to peroxisome proliferators. *Mol Pharmacol* **48:**559-567.

Inagaki T, Dutchak P, Zhao G, Ding X, Gautron L, Parameswara V, Li Y, Goetz R, Mohammadi M, Esser V, Elmquist JK, Gerard RD, Burgess SC, Hammer RE, Mangelsdorf DJ, and Kliewer SA (2007) Endocrine regulation of the fasting response by PPARαlpha-mediated induction of fibroblast growth factor 21. *Cell Metab* **5:**415-425.

Johnson DR, Guo GL, and Klaassen CD (2002) Expression of rat Multidrug Resistance Protein 2 (Mrp2) in male and female rats during normal and pregnenolone-16alpha-carbonitrile (PCN)-induced postnatal ontogeny. *Toxicology* **178:**209-219.

Johnson DR and Klaassen CD (2002a) Regulation of rat multidrug resistance protein 2 by classes of prototypical microsomal enzyme inducers that activate distinct transcription pathways. *Toxicol Sci* **67:**182-189.

Johnson DR and Klaassen CD (2002b) Role of rat multidrug resistance protein 2 in plasma and biliary disposition of dibromosulfophthalein after microsomal enzyme induction. *Toxicol Appl Pharmacol* **180:**56-63.

Kim D, Paggi JM, Park C, Bennett C, and Salzberg SL (2019) Graph-based genome alignment and genotyping with HISAT2 and HISAT-genotype. *Nat Biotechnol* **37:**907-915.

Klaassen CD (2002) Xenobiotic transporters: another protective mechanism for chemicals. *Int J Toxicol* **21:**7-12.

Klaassen CD and Aleksunes LM (2010) Xenobiotic, bile acid, and cholesterol transporters: function and regulation. *Pharmacol Rev* **62:**1-96.

Klaassen CD and Lu H (2008) Xenobiotic transporters: ascribing function from gene knockout and mutation studies. *Toxicol Sci* **101:**186-196.

Klaassen CD and Slitt AL (2005) Regulation of hepatic transporters by xenobiotic receptors. *Curr Drug Metab* **6:**309-328.

Knight TR, Choudhuri S, and Klaassen CD (2008) Induction of hepatic glutathione S-transferases in male mice by prototypes of various classes of microsomal enzyme inducers. *Toxicol Sci* **106:**329-338.

Krippner J, Falk S, Brunn H, Georgii S, Schubert S, and Stahl T (2015) Accumulation potentials of perfluoroalkyl carboxylic acids (PFCAs) and perfluoroalkyl sulfonic acids (PFSAs) in maize (Zea mays). *J Agric Food Chem* **63:**3646-3653.

Kudo N and Kawashima Y (2003) Induction of triglyceride accumulation in the liver of rats by perfluorinated fatty acids with different carbon chain lengths: comparison with induction of peroxisomal beta-oxidation. *Biol Pharm Bull* **26:**47-51.

Kudo N, Suzuki-Nakajima E, Mitsumoto A, and Kawashima Y (2006) Responses of the liver to perfluorinated fatty acids with different carbon chain length in male and female mice:in relation to induction of hepatomegaly, peroxisomal beta-oxidation and microsomal 1-acylglycerophosphocholine acyltransferase. *Biol Pharm Bull* **29:**1952-1957.

Kudo N, Yamazaki T, Sakamoto T, Sunaga K, Tsuda T, Mitsumoto A, and Kawashima Y (2011) Effects of perfluorinated fatty acids with different carbon chain length on fatty acid profiles of hepatic lipids in mice. *Biol Pharm Bull* **34:**856-864.

Langley AE (1990) Effects of perfluoro-n-decanoic acid on the respiratory activity of isolated rat liver mitochondria. *J Toxicol Environ Health* **29:**329-336.

Le Magueresse-Battistoni B, Vidal H, and Naville D (2018) Environmental Pollutants and Metabolic Disorders: The Multi-Exposure Scenario of Life. *Front Endocrinol (Lausanne)* **9:**582.

Lee DY and Kim EH (2019) Therapeutic Effects of Amino Acids in Liver Diseases: Current Studies and Future Perspectives. *J Cancer Prev* **24:**72-78.

Lehmann JM, Lenhard JM, Oliver BB, Ringold GM, and Kliewer SA (1997) Peroxisome proliferator-activated receptors alpha and gamma are activated by indomethacin and other non-steroidal anti-inflammatory drugs. *J Biol Chem* **272:**3406-3410.

Li CH, Shi YL, Li M, Guo LH, and Cai YQ (2020) Receptor-Bound Perfluoroalkyl Carboxylic Acids Dictate Their Activity on Human and Mouse Peroxisome Proliferator-Activated Receptor gamma. *Environ Sci Technol* **54:**9529-9536.

Li CY, Renaud HJ, Klaassen CD, and Cui JY (2016) Age-Specific Regulation of Drug-Processing Genes in Mouse Liver by Ligands of Xenobiotic-Sensing Transcription Factors. *Drug Metab Dispos* **44:**1038-1049.

Li H, Handsaker B, Wysoker A, Fennell T, Ruan J, Homer N, Marth G, Abecasis G, Durbin R, and Genome Project Data Processing S (2009) The Sequence Alignment/Map format and SAMtools. *Bioinformatics* **25:**2078-2079.

Lin L, Yee SW, Kim RB, and Giacomini KM (2015) SLC transporters as therapeutic targets: emerging opportunities. *Nat Rev Drug Discov* **14:**543-560.

Ling V and Thompson LH (1974) Reduced permeability in CHO cells as a mechanism of resistance to colchicine. *J Cell Physiol* **83:**103-116.

Liu B, Zhang H, Yao D, Li J, Xie L, Wang X, Wang Y, Liu G, and Yang B (2015) Perfluorinated compounds (PFCs) in the atmosphere of Shenzhen, China: Spatial distribution, sources and health risk assessment. *Chemosphere* **138:**511-518.

Louisse J, Rijkers D, Stoopen G, Janssen A, Staats M, Hoogenboom R, Kersten S, and Peijnenburg A (2020) Perfluorooctanoic acid (PFOA), perfluorooctane sulfonic acid (PFOS), and perfluorononanoic acid (PFNA) increase triglyceride levels and decrease cholesterogenic gene expression in human HepaRG liver cells. *Arch Toxicol* **94:**3137-3155.

Love MI, Huber W, and Anders S (2014) Moderated estimation of fold change and dispersion for RNA-seq data with DESeq2. *Genome Biol* **15:**550.

Lubrano C, Genovesi G, Specchia P, Costantini D, Mariani S, Petrangeli E, Lenzi A, and Gnessi L (2013) Obesity and metabolic comorbidities: environmental diseases? *Oxid Med Cell Longev* **2013:**640673.

Maher JM, Aleksunes LM, Dieter MZ, Tanaka Y, Peters JM, Manautou JE, and Klaassen CD (2008) Nrf2- and PPAR alpha-mediated regulation of hepatic Mrp transporters after exposure to perfluorooctanoic acid and perfluorodecanoic acid. *Toxicol Sci* **106:**319-328.

Maher JM, Cheng X, Slitt AL, Dieter MZ, and Klaassen CD (2005) Induction of the multidrug resistance-associated protein family of transporters by chemical activators of receptor-mediated pathways in mouse liver. *Drug Metab Dispos* **33:**956-962.

Maher JM, Cherrington NJ, Slitt AL, and Klaassen CD (2006) Tissue distribution and induction of the rat multidrug resistance-associated proteins 5 and 6. *Life Sci* **78:**2219-2225.

Mennone A, Soroka CJ, Cai SY, Harry K, Adachi M, Hagey L, Schuetz JD, and Boyer JL (2006) Mrp4-/- mice have an impaired cytoprotective response in obstructive cholestasis. *Hepatology* **43:**1013-1021.

Nath B and Szabo G (2012) Hypoxia and hypoxia inducible factors: diverse roles in liver diseases. *Hepatology* **55:**622-633.

Newman S and Guzelian PS (1982) Stimulation of de novo synthesis of cytochrome P-450 by phenobarbital in primary nonproliferating cultures of adult rat hepatocytes. *Proc Natl Acad Sci U S A* **79:**2922-2926.

Nies AT, Damme K, Schaeffeler E, and Schwab M (2012) Multidrug and toxin extrusion proteins as transporters of antimicrobial drugs. *Expert Opin Drug Metab Toxicol* **8:**1565-1577.

Oshida K, Vasani N, Jones C, Moore T, Hester S, Nesnow S, Auerbach S, Geter DR, Aleksunes LM, Thomas RS, Applegate D, Klaassen CD, and Corton JC (2015) Identification of chemical modulators of the constitutive activated receptor (CAR) in a gene expression compendium. *Nucl Recept Signal* **13:**e002.

Pan CJ, Chen SY, Jun HS, Lin SR, Mansfield BC, and Chou JY (2011) SLC37A1 and SLC37A2 are phosphate-linked, glucose-6-phosphate antiporters. *PLoS One* **6:**e23157.

Pannala VR, Estes SK, Rahim M, Trenary I, O'Brien TP, Shiota C, Printz RL, Reifman J, Shiota M, Young JD, and Wallqvist A (2020) Toxicant-Induced Metabolic Alterations in Lipid and Amino Acid Pathways Are Predictive of Acute Liver Toxicity in Rats. *Int J Mol Sci* **21**.

Pasanisi E, Cortes-Gomez AA, Perez-Lopez M, Soler F, Hernandez-Moreno D, Guerranti C, Martellini T, Fuentes-Mascorro G, Romero D, and Cincinelli A (2016) Levels of perfluorinated acids (PFCAs) in different tissues of Lepidochelys olivacea sea turtles from the Escobilla beach (Oaxaca, Mexico). *Sci Total Environ* **572:**1059-1065.

Pedersen PL (2005) Transport ATPases: structure, motors, mechanism and medicine: a brief overview. *J Bioenerg Biomembr* **37:**349-357.

Rausch-Derra LC, Hartley DP, Meier PJ, and Klaassen CD (2001) Differential effects of microsomal enzyme-inducing chemicals on the hepatic expression of rat organic anion transporters, OATP1 and OATP2. *Hepatology* **33:**1469-1478.

Rockwell CE, Turley AE, Cheng X, Fields PE, and Klaassen CD (2013) Acute Immunotoxic Effects of Perfluorononanoic Acid (PFNA) in C57BL/6 Mice. *Clin Exp Pharmacol* **Suppl 4**.

Rockwell CE, Turley AE, Cheng X, Fields PE, and Klaassen CD (2017) Persistent alterations in immune cell populations and function from a single dose of perfluorononanoic acid (PFNA) in C57Bl/6 mice. *Food Chem Toxicol* **100:**24-33.

Ruggiero, M.J.; Miller, H.; Idowu, J.Y.; Zitzow, J.D.; Chang, S.-C.; Hagenbuch, B. Perfluoroalkyl Carboxylic Acids Interact with the Human Bile Acid Transporter NTCP. Livers 2021, 1, 221–229. https:// doi.org/10.3390/livers1040017

Sagami F, Tsukidate K, Fukuda T, Nakanowatari J, Horie T, Igarashi T, Kitada M, and Kanakubo Y (1990) Induction and immunohistochemical localization of cytochrome P-450 PCN by non-steroidal compound, in rat liver microsomes. *Res Commun Chem Pathol Pharmacol* **67:**79-86.

Saito C, Zwingmann C, and Jaeschke H (2010) Novel mechanisms of protection against acetaminophen hepatotoxicity in mice by glutathione and N-acetylcysteine. *Hepatology* **51:**246-254.

Schlezinger JJ, Puckett H, Oliver J, Nielsen G, Heiger-Bernays W, and Webster TF (2020) Perfluorooctanoic acid activates multiple nuclear receptor pathways and skews expression of genes regulating cholesterol homeostasis in liver of humanized PPARαlpha mice fed an American diet. *Toxicol Appl Pharmacol* **405:**115204.

Schmidt A, Endo N, Rutledge SJ, Vogel R, Shinar D, and Rodan GA (1992) Identification of a new member of the steroid hormone receptor superfamily that is activated by a peroxisome proliferator and fatty acids. *Mol Endocrinol* **6:**1634-1641.

Shelby MK and Klaassen CD (2006) Induction of rat UDP-glucuronosyltransferases in liver and duodenum by microsomal enzyme inducers that activate various transcriptional pathways. *Drug Metab Dispos* **34:**1772-1778.

Sinclair E, Mayack DT, Roblee K, Yamashita N, and Kannan K (2006) Occurrence of perfluoroalkyl surfactants in water, fish, and birds from New York State. *Arch Environ Contam Toxicol* **50:**398-410.

Slitt AL, Cherrington NJ, Maher JM, and Klaassen CD (2003) Induction of multidrug resistance protein 3 in rat liver is associated with altered vectorial excretion of acetaminophen metabolites. *Drug Metab Dispos* **31:**1176-1186.

Smithwick M, Muir DC, Mabury SA, Solomon KR, Martin JW, Sonne C, Born EW, Letcher RJ, and Dietz R (2005) Perflouroalkyl contaminants in liver tissue from East Greenland polar bears (Ursus maritimus). *Environ Toxicol Chem* **24:**981-986.

Staels B, Koenig W, Habib A, Merval R, Lebret M, Torra IP, Delerive P, Fadel A, Chinetti G, Fruchart JC, Najib J, Maclouf J, and Tedgui A (1998) Activation of human aortic smooth-muscle cells is inhibited by PPARαlpha but not by PPARgamma activators. *Nature* **393:**790-793.

Tajiri K and Shimizu Y (2018) Branched-chain amino acids in liver diseases. *Transl Gastroenterol Hepatol* **3:**47.

Takagi A, Sai K, Umemura T, Hasegawa R, and Kurokawa Y (1991) Short-term exposure to the peroxisome proliferators, perfluorooctanoic acid and perfluorodecanoic acid, causes significant increase of 8-hydroxydeoxyguanosine in liver DNA of rats. *Cancer Lett* **57:**55-60.

Van Rafelghem MJ, Mattie DR, Bruner RH, and Andersen ME (1987) Pathological and hepatic ultrastructural effects of a single dose of perfluoro-n-decanoic acid in the rat, hamster, mouse, and guinea pig. *Fundam Appl Toxicol* **9:**522-540.

Vanden Heuvel JP, Kuslikis BI, Van Rafelghem MJ, and Peterson RE (1991a) Disposition of perfluorodecanoic acid in male and female rats. *Toxicol Appl Pharmacol* **107:**450-459.

Vanden Heuvel JP, Kuslikis BI, Van Rafelghem MJ, and Peterson RE (1991b) Tissue distribution, metabolism, and elimination of perfluorooctanoic acid in male and female rats. *J Biochem Toxicol* **6:**83-92.

Vanden Heuvel JP, Thompson JT, Frame SR, and Gillies PJ (2006) Differential activation of nuclear receptors by perfluorinated fatty acid analogs and natural fatty acids: a comparison of human, mouse, and rat peroxisome proliferator-activated receptor-alpha, -

beta, and -gamma, liver X receptor-beta, and retinoid X receptor-alpha. *Toxicol Sci* **92:**476-489.

Vansell NR and Klaassen CD (2002) Increase in rat liver UDP-glucuronosyltransferase mRNA by microsomal enzyme inducers that enhance thyroid hormone glucuronidation. *Drug Metab Dispos* **30:**240-246.

Wang J, Yan S, Zhang W, Zhang H, and Dai J (2015) Integrated proteomic and miRNA transcriptional analysis reveals the hepatotoxicity mechanism of PFNA exposure in mice. *J Proteome Res* **14:**330-341.

Watkins JB and Klaassen CD (1983) Chemically-induced alteration of UDP-glucuronic acid concentration in rat liver. *Drug Metab Dispos* **11:**37-40.

Wen X, Baker AA, Klaassen CD, Corton JC, Richardson JR, and Aleksunes LM (2019) Hepatic carboxylesterases are differentially regulated in PPARαlpha-null mice treated with perfluorooctanoic acid. *Toxicology* **416:**15-22.

Yang B, Zou W, Hu Z, Liu F, Zhou L, Yang S, Kuang H, Wu L, Wei J, Wang J, Zou T, and Zhang D (2014) Involvement of oxidative stress and inflammation in liver injury caused by perfluorooctanoic acid exposure in mice. *Biomed Res Int* **2014:**409837.

Yang K, Koh KH, and Jeong H (2010) Induction of CYP2B6 and CYP3A4 expression by 1-aminobenzotriazole (ABT) in human hepatocytes. *Drug Metab Lett* **4:**129-133.

Yonezawa A and Inui K (2011) Importance of the multidrug and toxin extrusion MATE/SLC47A family to pharmacokinetics, pharmacodynamics/toxicodynamics and pharmacogenomics. *Br J Pharmacol* **164:**1817-1825.

Zhang Y, Cheng X, Aleksunes L, and Klaassen CD (2012) Transcription factor-mediated regulation of carboxylesterase enzymes in livers of mice. *Drug Metab Dispos* **40:**1191-1197.Zhang Y, Zhang Y, Klaassen CD, and Cheng X (2018) Alteration of Bile Acid and Cholesterol Biosynthesis and Transport by Perfluorononanoic Acid (PFNA) in Mice. *Toxicol Sci* **162:**225-233.

Zhao W, Zitzow JD, Weaver Y, Ehresman DJ, Chang SC, Butenhoff JL, and Hagenbuch B (2017) Organic Anion Transporting Polypeptides Contribute to the Disposition of Perfluoroalkyl Acids in Humans and Rats. *Toxicol Sci* **156:**84-95.

ACKNOWLEDGEMENTS:

The authors would like to thank members of the Cui Laboratory for editing the manuscript.

AUTHORSHIP CONTRIBUTIONS:

Participated in research design: Cui.

Conducted experiments: Lim, Suh, and Cui.

Contributed new reagents or analytic tools: N/A.

Performed data analysis: Lim, Suh, and Cui.

Wrote or contributed to the writing of the manuscript: Lim, Suh, Faustman, and Cui.

FOOTNOTES:

Supported by National Institutes of Health (NIH) grants [R01ES025708, R01ES030197, R01GM111381, R01ES031098], the University of Washington Center for Exposures, Diseases, Genomics, and Environment [P30ES007033], Environmental Pathology/Toxicology Training Program [T32ES007032], the University of Washington Sheldon Murphy Endowment, and the University of Washington Environmental Health and Microbiome Research (EHMiR) Center (DEOHS). All authors declared no financial conflict of interests.